


Model of localized state mediated exchange interaction and ferromagnetism in diluted magnetic semiconductors

I. A. Kokurin^{1,2,*} and N. S. Averkiev¹

¹*Ioffe Institute, 194021 St. Petersburg, Russia*

²*Institute of High Technologies and New Materials, National Research Ogarev Mordovia State University, 430005 Saransk, Russia*

 (Received 31 December 2023; revised 10 April 2024; accepted 23 May 2024; published 11 June 2024)

The real mechanism of ferromagnetism in diluted magnetic semiconductors (DMSs), in particular in GaMnAs, is not yet fully understood. The well-known Ruderman-Kittel-Kasuya-Yosida (RKKY) interaction, mediated by itinerant charge carriers, is accepted to be responsible for the ferromagnetism in GaMnAs in its metallic state. At the same time, GaMnAs can be realized in an insulating state when there are no mobile carriers, and holes are localized at acceptors. At not too low Mn concentration, the overlap of acceptor-wave-function tails can be sufficient, and Mn d shells can be aligned by means of indirect mechanism mediated by localized holes. An increase in the content of Mn ions leads to their incorporation into interstitial positions, which in turn leads to self-compensation, i.e., the number of localized holes per paramagnetic center decreases. This means that the pairwise interaction of d shells can be mediated by two holes as well as single hole. In order to study the microscopic mechanism of indirect exchange, the energy and spin structure of molecule-like complexes with one and two charge carriers, localized by field of two paramagnetic ions, is investigated. It is shown that at short interionic distances (high concentration of magnetic component) the established mechanisms of indirect exchange resemble the well-known mechanisms of double- and superexchange with ferro- and antiferromagnetic alignment of magnetic moments, respectively. However, these results that can be found perturbatively, are significantly modified when the interionic distance R increases. Our calculations show that the magnetic ordering in insulating DMS crystal significantly depends not only on the concentration of magnetic component but on the compensation degree as well: cases of low or total compensation correspond to the absence of any magnetic ordering, whereas, the pronounced ferromagnetism is realized at a compensation degree close to a half. The simple estimate for the Curie temperature is derived in the limit of half-compensation.

DOI: [10.1103/PhysRevB.109.214415](https://doi.org/10.1103/PhysRevB.109.214415)

I. INTRODUCTION

Diluted magnetic semiconductors (DMSs), such as GaMnAs, attract attention due to their interesting magnetic properties and the ability to integrate with conventional semiconductor (and even silicon) electronics. In GaMnAs usually the indirect exchange interaction in the spirit of Zener [1] or Ruderman-Kittel-Kasuya-Yosida (RKKY) [2–4] models is accepted to be responsible for ferromagnetism [5,6]. However, this consideration is valid when the manganese content is several percent, and the exchange is mediated by itinerant holes. At the same time, it is of interest to consider ferromagnetism in DMS in an insulating state. In this case, indirect exchange occurs due to the overlap of the wave functions of holes localized directly on paramagnetic acceptors. The realization of metallic or insulating state depends not only on the Mn content, but on the growth conditions as well. The specifics of low-temperature growth leads to the compensation, due to interstitial atoms Mn_I [7,8] and arsenic antisites As_{Ga} . At the same total Mn content the insulating phase appears at lower substrate temperatures; the corresponding phase diagram is presented in Ref. [9].

The ferromagnetism in the insulating state is noticeably weaker and the Curie temperature is lower (up to tens of Kelvin [10–12]). Insulating samples can find applications e.g., in superconducting spintronics, more precisely, in hybrid ferromagnet/superconductor (F/S) structures [13] (see also recent review [14] and references therein). In this case, the low Curie temperature is not so critical, since low temperatures are also required for the existence of superconductivity. The use of the ferromagnetic insulator instead of a ferromagnetic metal in hybrid F/S system is preferable because the proximity effect that destroys superconductivity, is limited to the interface as the electron wave function decays in an insulator on atomic scales [15]. This was discussed by de Gennes more than half a century ago [16].

GaAs doped with Mn at low content (up to 10^{17} cm⁻³), when the interaction between magnetic impurities is negligible, is studied very well. In this case, the Mn²⁺ ion is embedded into GaAs crystal lattice, substituting the Ga cation. The usual notation is used for substitutional Mn impurity Mn_{Ga} . Because of the lack of one electron, Mn_{Ga} acts as an acceptor, i.e., it binds a hole. In addition, Mn inner d shell with total spin of $S = 5/2$ is antiferromagnetically aligned with the hole total angular momentum $J = 3/2$ (see, for instance, review [17] and references therein). This coupling provides a direct access to the Mn spin through photoneutralization of

*ivan.a.kokurin@gmail.ru

impurities (excitation with energies below the gap) by circularly polarized light in compensated semiconductors [18,19].

The interaction of impurities becomes important at definite concentration, which depends on the spatial extent of localized-carrier wave function. It has recently been shown that the interaction between impurities and the formation of multicenter impurity complexes can manifest themselves in optical phenomena. In particular, the broadening of long-wave tail of the acceptor-related photoluminescence line is explained [20,21]. For deeper impurities, such as Mn, higher concentration is needed to test the interaction between them. The interaction of paramagnetic impurities leads to intriguing phenomena. A possibility to change the magnitude and the sign of the electron magnetization in Mn-doped GaAs structures by optical means alone has been recently predicted [22].

Consideration of any mechanism of magnetic ordering usually begins with the study of a pair exchange interaction. An increase in the content of the magnetic component leads to overlapping of the wave functions of holes of neutral magnetic acceptors Mn_{Ga}^0 . Thus, it is necessary to consider the energy and spin structure of two interacting magnetic acceptors or, in other words, the Mn_2^0 molecule-like complex. At the same time, it is well known that an attempt to increase the Mn content in GaAs leads to incorporation of Mn ions into interstitial positions [23]. In this case, Mn behaves like a double donor that in turn leads to self-compensation. The latter decreases the number of localized holes per paramagnetic center. Thus, it is important to know the mechanism of interaction not only between two neutral Mn_{Ga}^0 acceptors (Mn_2^0 complex), but also between a neutral acceptor Mn_{Ga}^0 and an ionized Mn_{Ga}^- one (Mn_2^- complex). Eventually, the calculation of the energy levels and spin structure of the Mn_2^- and Mn_2^0 complexes is the first step towards understanding the indirect exchange interaction and ferromagnetism in $\text{Ga}_{1-x}\text{Mn}_x\text{As}$ in the insulating state.

In Ref. [24] an interaction of a pair of substitutional Mn impurities in GaAs was considered within the tight-binding model. It should be noted, however, that the effect of compensation was not taken into account, i.e., the interaction of neutral and ionized acceptors was not considered. The ferromagnetism in GaMnAs has been modeled within the mean-field [25,26] and Monte Carlo [27,28] simulations. However, at that time there was no established point of view that Mn interstitials are responsible for compensation.

Usually, both for RKKY and localized-carrier-mediated [24] exchange interaction the following procedure is used to find the strength of indirect exchange: two collinear configurations with parallel and antiparallel d -shell spins are considered, and the energy difference of ground states with above spin configurations is defined as the exchange parameter. In this case, the actual magnitude of the d -shell spin is not very important. On the contrary, we will consider a completely quantum problem, where the inner electron shell enters the problem not as a classical object, but as a quantum one.

The problem will be solved using the language of the semiconductor physics. This means using methods that are typical in the field, such as the effective mass approximation. It is assumed that the spectral problem for Mn^0 is solved within the framework of this method. The hole ground state, corresponding to the total angular momentum of $J = 3/2$ with a level

near the valence band of Γ_8 symmetry, is fourfold degenerate [29,30]. The additional sixfold degeneracy corresponds to the effective d -shell spin $S = 5/2$. Thus, the level structure of Mn^0 acceptor is described by $4 \times 6 = 24$ basis functions, and the degeneracy is partially lifted by isotropic exchange interaction, $\propto \mathbf{J} \cdot \mathbf{S}$. The states are classified according to the total angular momentum $\mathbf{F} = \mathbf{J} + \mathbf{S}$.

In the case of pair complexes, Mn_2^- and Mn_2^0 , the number of states that should be taken into account is equal to the product of the number of possible states of d -shell pair ($6 \times 6 = 36$) and the number of hole states in nonmagnetic acceptor complexes A_2^- or A_2^0 . In the simpler case of the complex A_2^- there are eight pairwise degenerate states [20,31]. This means that the spectral problem for the Mn_2^- complex includes $8 \times 36 = 288$ basis states. The A_2^0 complex should be described by $C_8^2 = \frac{8!}{6!2!} = 28$ two-hole basis functions [31]. As a result, to describe the Mn_2^0 complex it is necessary to use $28 \times 36 = 1008$ basis states.

The consideration of above Mn_2^- and Mn_2^0 complexes is difficult. Here simpler models will be considered: it is assumed that the spins of both localized carriers and inner magnetic shells have a minimal value of $1/2$, and the complexes have shallow levels near a simple band with an isotropic effective mass. These assumptions significantly simplify the problems. We will call the simplified complexes with one and two charge carriers D_2^- and D_2^0 , respectively, since they are more similar to donor-like complexes in GaAs with levels close to the isotropic conduction band of Γ_6 symmetry.

The paper is organized as follows. Section II contains the results for the spectral problems corresponding to one and two electrons bounded at two donors (nonmagnetic D_2^- and D_2^0 complexes). The intracenter exchange interaction is introduced and the spectral problems for magnetic D_2^- and D_2^0 complexes are solved in Sec. III. The spin structure of magnetic D_2^- and D_2^0 complexes is considered and the specifics of indirect exchange interaction in GaMnAs is discussed in Sec. IV. A brief summary of the results is presented in Sec. V. Some calculation details are presented in Appendices A–D.

II. STRUCTURE OF NONMAGNETIC TWO-CENTER COMPLEXES

Let us remind the structure of nonmagnetic D_2^+ and D_2^0 complexes. Here an isotropic scalar effective mass is used. In this approximation the spectral problems for D_2^+ and D_2^0 nonmagnetic complexes coincide with that for H_2^+ ion and H_2 molecule, respectively, up to renormalization of dielectric screening and effective mass. It should be noted that the H_2^+ (D_2^+) problem can be solved exactly [32–34]. However, these numerical results do not allow further consideration of the magnetic complex. For this reason the approximate methods, known in quantum chemistry, are used.

The spectral problems are solved within the framework of *molecular orbitals* (MOs) approach (see, for instance, Ref. [34]), which is applied to the envelope functions of charge carriers in a semiconductor crystal. MOs are presented as *linear combination of atomic orbitals* (LCAOs). In our case, the *atomic orbitals* (AOs) correspond to envelope wave functions of single acceptor (donor). Only the ground-state wave functions are used as AOs: hydrogen-like $1s$ function is

given by

$$\phi(r) = \frac{a^{3/2}}{\sqrt{\pi}} e^{-ar}, \quad (1)$$

where a is a dimensionless variational parameter. Hereinafter, for the sake of simplicity, dimensionless lengths are used: the effective Bohr radius $a_B = \varepsilon \hbar^2 / me^2$ is the corresponding unit of length. Above function is eigenfunction of hydrogen-like Hamiltonian $H_0 = -\nabla^2 - \frac{2}{r}$ and corresponds to the ground-state energy -1 . The Hamiltonian and corresponding energy eigenvalue are dimensionless as well: the effective Rydberg $E_0 = me^4 / 2\varepsilon^2 \hbar^2$ is the corresponding energy unit. Here m is the electron effective mass and ε is the static dielectric constant of semiconductor crystal.

In quantum chemistry, the variational method is usually used to improve the accuracy of calculations (see, for instance, Ref. [32]). However, in our approach the variational procedure is neglected, and the variational parameter is simply set to $a = 1$. Such a simplification does not affect the main qualitative results, whereas taking into account the a dependence significantly complicates the calculations. Moreover, the variational procedure is not applicable to magnetic complexes. This is due to the fact that the exchange-dependent part of the energy is proportional to the higher powers of the variation parameter ($\propto a^3$). It should be noted that when considering a simplified model, we are trying to find qualitative features, rather than carry out a strict quantitative calculation.

A. Nonmagnetic D_2^+ complex

Now let us consider the spectral problem for the single-electron nonmagnetic D_2^+ complex. Two positively charged ions are located at points A and B , separated by a distance R , with position vectors $\mathbf{R}_{A(B)} = (0, 0, \mp R/2)$. Two ion-to-electron position vectors $\mathbf{r}_{A(B)} = \mathbf{r} - \mathbf{R}_{A(B)}$ should be introduced into the problem. The single-particle Hamiltonian includes the electron kinetic term, the potential energy of attraction by centers A and B , and interionic repulsion,

$$H^{D_2^+} = -\nabla^2 - \frac{2}{r_A} - \frac{2}{r_B} + \frac{2}{R}. \quad (2)$$

The permutation symmetry of the problem leads to the following form of the normalized MO-like wave function,

$$\psi_p(\mathbf{r}) = \frac{1}{\sqrt{2(1+pS)}} [\phi(r_A) + p\phi(r_B)], \quad (3)$$

which is symmetric ($p = +$) or antisymmetric ($p = -$) relative to the permutation of ions ($A \leftrightarrow B$). Here $S = \int d\tau \phi(r_A)\phi(r_B)$ is the overlap integral.

Calculation of the matrix elements of the Hamiltonian (2) between wave functions (3) gives the eigenenergies

$$E_{\pm}(R) = -1 + \frac{2}{R} - \frac{j'(R) \pm k'(R)}{1 \pm S(R)}, \quad (4)$$

corresponding to ψ_{\pm} states, respectively. Here $j'(R) = \langle \phi_A | \frac{2}{r_B} | \phi_A \rangle$ and $k'(R) = \langle \phi_A | \frac{2}{r_A} | \phi_B \rangle$ are Coulomb and resonance integral, respectively, where the notation $\phi_i \equiv \phi(r_i)$ ($i = A, B$) is used. The explicit form of overlap S , Coulomb j' , and resonance k' integrals is presented in Appendix A. An additive term $\frac{2}{R}$ is introduced into Eq. (4) as a reminder that

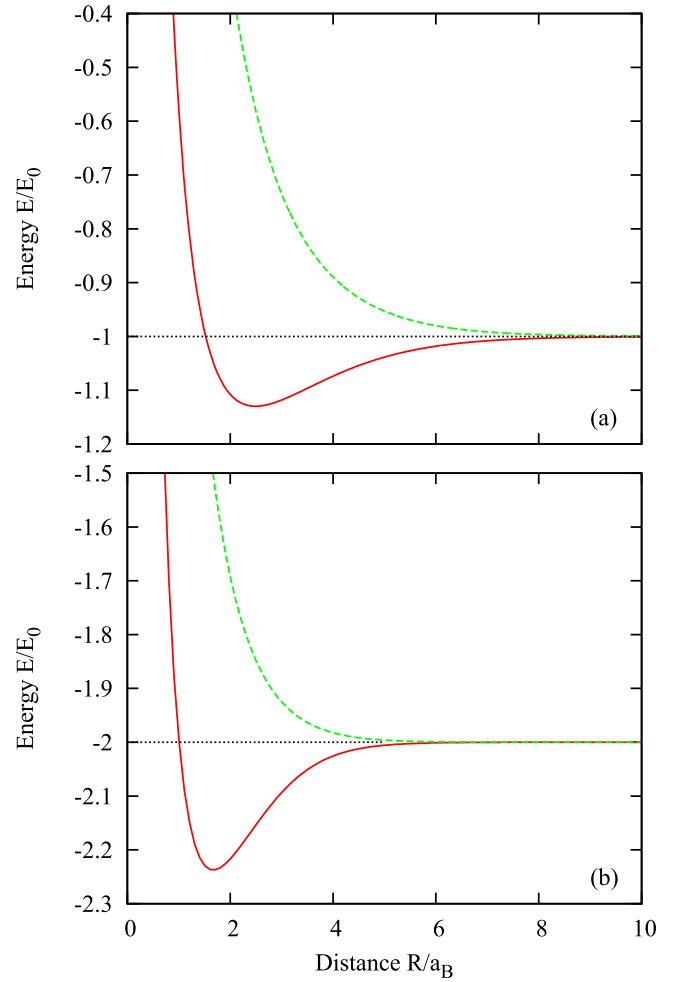


FIG. 1. Dependence of energy levels on interionic distance R . (a) Nonmagnetic complex D_2^+ . Solid-red (dashed-green) line corresponds to E_+ (E_-) level. (b) Nonmagnetic complex D_2^0 . Solid-red (dashed-green) line corresponds to E_s (E_t) level.

complexes with small R are not formed in the crystal due to interionic repulsion.

The dependence of energy levels E_{\pm} of D_2^+ complex on the interionic distance R is shown in Fig. 1(a). The ground state corresponds to the energy E_+ , and the energy of excited level is E_- .

B. Nonmagnetic D_2^0 complex

Now consider the spectral problem for the nonmagnetic D_2^0 complex. The Hamiltonian, taking into account the attraction of both electrons 1 and 2 to both ions A and B , as well as interelectronic and interionic repulsion, is given by

$$H^{D_2^0} = -\nabla_1^2 - \nabla_2^2 - \sum_{i=1,2} \sum_{j=A,B} \frac{2}{r_{ij}} + \frac{2}{r_{12}} + \frac{2}{R}. \quad (5)$$

Here the electron position vectors relative to ion $A(B)$ are introduced, $\mathbf{r}_{ij} = \mathbf{r}_i - \mathbf{R}_j$ with $i = 1, 2$ and $j = A, B$; the vector $\mathbf{r}_{12} = \mathbf{r}_1 - \mathbf{r}_2$ corresponds to the interelectron distance.

The solution of the spectral problem is considered in the MO-LCAO [35] scheme as well. Using the single-electron

two-center wave functions (3) the two-particle wave functions of orbital motion satisfying the permutation conditions can be written in the form

$$\Psi_1(1, 2; {}^1\Sigma_g) = \psi_+(\mathbf{r}_1)\psi_+(\mathbf{r}_2), \quad (6a)$$

$$\Psi_2(1, 2; {}^3\Sigma_u) = \frac{1}{\sqrt{2}}[\psi_+(\mathbf{r}_1)\psi_-(\mathbf{r}_2) - \psi_-(\mathbf{r}_1)\psi_+(\mathbf{r}_2)], \quad (6b)$$

$$\Psi_3(1, 2; {}^1\Sigma_u) = \frac{1}{\sqrt{2}}[\psi_+(\mathbf{r}_1)\psi_-(\mathbf{r}_2) + \psi_-(\mathbf{r}_1)\psi_+(\mathbf{r}_2)], \quad (6c)$$

$$\Psi_4(1, 2; {}^1\Sigma_g) = \psi_-(\mathbf{r}_1)\psi_-(\mathbf{r}_2). \quad (6d)$$

Here the molecular-physics notations are used (see, for instance, Ref. [34]): the Greek Σ corresponds to zero projection of the orbital angular momentum onto the intercenter axis, $L_z = 0$; the subscript denotes the parity with respect to electron permutations (g for even and u for odd); a superscript denotes the multiplicity (singlet/triplet) corresponding to the spin state of two electrons.

By calculating the matrix elements of the Hamiltonian (5) between wave functions (6), and taking into account that the functions ψ_{\pm} (3) for electron 1 or 2 are the solutions of the Schrödinger equation with the Hamiltonian (2), we find the energy levels of D_2^0 complex. It should be taken into account that the symmetry of the functions (6) is following: only states Ψ_1 and Ψ_4 are mixed by the term describing the interelectron repulsion.

The spectral problem for the Hamiltonian block 2×2

$$H = \begin{pmatrix} H_{11} & H_{14} \\ H_{41} & H_{44} \end{pmatrix}, \quad (7)$$

written relative to the basis functions Ψ_1 and Ψ_4 , has a standard solution,

$$E_{1,4} = \frac{H_{11} + H_{44}}{2} \mp \sqrt{\left(\frac{H_{44} - H_{11}}{2}\right)^2 + H_{14}^2}, \quad (8)$$

where

$$H_{11} = 2E_+ + \frac{2}{R} + \frac{m + j + 4l + 2k}{2(1 + S)^2}, \quad (9)$$

$$H_{44} = 2E_- + \frac{2}{R} + \frac{m + j - 4l + 2k}{2(1 - S)^2}, \quad (10)$$

$$H_{14} = H_{41} = \frac{m - j}{2(1 - S^2)}. \quad (11)$$

The energies of second and third levels are given by

$$E_2 = \langle \Psi_2 | H^{D_2^0} | \Psi_2 \rangle = E_+ + E_- + \frac{2}{R} + \frac{j - k}{1 - S^2}, \quad (12)$$

$$E_3 = \langle \Psi_3 | H^{D_2^0} | \Psi_3 \rangle = E_+ + E_- + \frac{2}{R} + \frac{m - k}{1 - S^2}. \quad (13)$$

All matrix elements and energies of D_2^0 complex are expressed in terms of the energies $E_{\pm}(R)$ and four integrals j , k , l , and m , which known as Coulomb, exchange, hybrid, and single-center integral, respectively. The explicit form of these integrals is presented in Appendix B.

The dependencies of the energy levels E_1 and E_2 on intercenter distance R are depicted in Fig. 1(b). The E_3 and E_4 levels have energies approximately E_0 higher. In the further consideration of the magnetic D_2^0 complex, they are not taken into account, since the energy of the exchange interaction between the magnetic moment of each electron and the magnetic moment of the inner shell of each ion is much less than the energy distance to these levels. Moreover, the energies of these levels are found with less accuracy within the MO approximation.

The wave functions corresponding to E_1 and E_2 levels are given by

$$\Phi_1(1, 2; {}^1\Sigma_{g1}) = \cos \frac{\theta}{2} \Psi_1(1, 2; {}^1\Sigma_g) - \sin \frac{\theta}{2} \Psi_4(1, 2; {}^1\Sigma_g), \quad (14a)$$

$$\Phi_2(1, 2; {}^3\Sigma_u) = \Psi_2(1, 2; {}^3\Sigma_u), \quad (14b)$$

where $\tan \theta = 2H_{14}/(H_{44} - H_{11})$.

The wave functions Φ_3 and Φ_4 are not written down here, since they are not used in further consideration. However, it is obvious that $\Phi_3 = \Psi_3$ and Φ_4 can be written as a linear combination of the same functions as in Φ_1 with coefficients ensuring the orthogonality of Φ_1 and Φ_4 . Here and below, the levels E_1 and E_2 are designated as E_s and E_t , respectively (the subscripts correspond to singlet and triplet).

III. STRUCTURE OF MAGNETIC TWO-CENTER COMPLEXES

The exchange interaction between the spin of the charge carrier and the magnetic moment of the inner shell (say, the d shell of a transition metal ion) is usually described by the Heisenberg-like Hamiltonian [36]

$$H_{ex} = -\mathcal{J}(|\mathbf{r} - \mathbf{R}|)\mathbf{s} \cdot \mathbf{S}, \quad (15)$$

where \mathbf{s} is the spin operator of a bound carrier. The simplest case of an electron with spin $s = 1/2$ is considered here. Thus, corresponding spin operator is expressed in terms of Pauli matrices $\boldsymbol{\sigma} = (\sigma_x, \sigma_y, \sigma_z)$, $\mathbf{s} = \frac{1}{2}\boldsymbol{\sigma}$. The explicit form of the magnetic-shell spin operator \mathbf{S} depends on the specific value of S . In our model it is equal to $1/2$, i.e., it is expressed in terms of Pauli matrices as well, $\mathbf{S} = \frac{1}{2}\boldsymbol{\sigma}$. The strength of exchange interaction is described by $\mathcal{J}(r)$, which is generally considered to be spherically symmetrical and its extent is of atomic scale. Here \mathbf{r} and \mathbf{R} are the position vectors of the electron and the magnetic-shell spin, respectively.

The use of the envelope function approximation (EFA) means that the electron wave function can be presented as a product of the Bloch function of the corresponding extremum and the envelope function, which slowly varies at the scale of a lattice constant. This decomposition allows one to calculate the matrix element of the exchange operator between the electron wave functions. Integration of the operator (15) with the squared electron ground-state wave function (1), pre-multiplied by the s -type Bloch function, taking into account EFA decomposition and short-range form of $\mathcal{J}(r)$, leads to the spin representation of exchange operator [37]

$$H_{ex} = -As \cdot S, \quad (16)$$

where $A = \alpha\phi^2(0) = \frac{\alpha}{\pi}$ is an exchange constant. Thus, the intracenter exchange constant A is related to the band exchange parameter α , which in the case of simple band of Γ_6 symmetry is given by

$$\alpha = \int_{\Omega} d^3r \mathcal{J}(r) |\mathcal{S}|^2.$$

Here \mathcal{S} is the s -like Bloch function of Γ_6 band bottom. The integration in the above equation is carried out over the volume Ω of the unit cell. The donor ground state splits into states with different values of the total angular momentum $\mathbf{F} = \mathbf{s} + \mathbf{S}$,

$$\Delta E_F = -\frac{A}{2} \left[F(F+1) - \frac{3}{2} \right], \quad (17)$$

and for $F = 0$ (singlet) and $F = 1$ (triplet) the energy shift is equal to

$$\Delta E_{F=0} = \frac{3A}{4}, \quad \Delta E_{F=1} = -\frac{A}{4}. \quad (18)$$

$$\langle p', \mu', \lambda', \nu' | H_{ex}^{D_2^+} | p, \mu, \lambda, \nu \rangle = -\frac{\alpha}{4} \left[\sum_{j=x,y,z} N_{p'p}(0, R) (\sigma_j)_{\mu'\mu} (\sigma_j)_{\lambda'\lambda} \delta_{\nu'\nu} + \sum_{j=x,y,z} N_{p'p}(R, 0) (\sigma_j)_{\mu'\mu} \delta_{\lambda'\lambda} (\sigma_j)_{\nu'\nu} \right],$$

where $\delta_{x'x}$ is the Kronecker delta and $N_{p'p}(r_A, r_B) = \psi_{p'}(r_A, r_B) \psi_p(r_A, r_B)$. The latter is included into matrix element in the form

$$N_{p'p}(0, R) = p' p N_{p'p}(R, 0) = \frac{(1 + p'e^{-R})(1 + pe^{-R})}{2\pi \sqrt{[1 + p'S(R)][1 + pS(R)]}}.$$

Thus, the matrix of exchange Hamiltonian (19) is given by

$$H_{ex}^{D_2^+} = -\frac{1}{4} \begin{pmatrix} P \sum_{j=x,y,z} (\sigma_j \otimes \tau_j \otimes \chi_0 + \sigma_j \otimes \tau_0 \otimes \chi_j) & D \sum_{j=x,y,z} (\sigma_j \otimes \tau_j \otimes \chi_0 - \sigma_j \otimes \tau_0 \otimes \chi_j) \\ D \sum_{j=x,y,z} (\sigma_j \otimes \tau_j \otimes \chi_0 - \sigma_j \otimes \tau_0 \otimes \chi_j) & M \sum_{j=x,y,z} (\sigma_j \otimes \tau_j \otimes \chi_0 + \sigma_j \otimes \tau_0 \otimes \chi_j) \end{pmatrix}, \quad (20)$$

where σ_i , τ_i , and χ_i ($i = x, y, z$) are the Pauli matrices acting on the spins s , S^A , and S^B , respectively. The matrices σ_0 , τ_0 , and χ_0 are the 2×2 identity matrices. Three types of exchange parameters are introduced here,

$$P(R) = \alpha N_{++}(0, R) = \frac{A(1 + e^{-R})^2}{2[1 + S(R)]}, \quad (21a)$$

$$M(R) = \alpha N_{--}(0, R) = \frac{A(1 - e^{-R})^2}{2[1 - S(R)]}, \quad (21b)$$

$$D(R) = \alpha N_{+-}(0, R) = \frac{A(1 - e^{-2R})}{2\sqrt{1 - S^2(R)}}. \quad (21c)$$

The dependence of exchange parameters on the interionic distance R is depicted in Fig. 2. At large R all parameters tend to the value $A/2$, whereas at $R \rightarrow 0$ they are: $P(0) = A$, $M(0) = 3A$, $D(0) = \sqrt{3}A$.

The nonexchange part of the total Hamiltonian, which should be summed with $H_{ex}^{D_2^+}$, is given by $\langle p', \mu', \lambda', \nu' | H^{D_2^+} | p, \mu, \lambda, \nu \rangle = E_p \delta_{p'p} \delta_{\mu'\mu} \delta_{\lambda'\lambda} \delta_{\nu'\nu}$.

It can be seen that the intracenter exchange interaction resembles the hyperfine interaction in the ground state of the hydrogen atom, caused by the Fermi contact term.

A. Magnetic D_2^+ complex

Let us consider the level structure of the magnetic D_2^+ complex. In this case, the electron is bound by the field of two ions, each of which has an inner shell with nonzero spin. In this case, the inclusion of the following Heisenberg-type operator in the Hamiltonian is required,

$$H_{ex}^{D_2^+} = - \sum_{j=A,B} \mathcal{J}(|\mathbf{r} - \mathbf{R}_j|) \mathbf{s} \cdot \mathbf{S}^j, \quad (19)$$

where the exchange interaction of the electron spin \mathbf{s} with the spins of the inner shells of both paramagnetic ions A and B is taken into account. The direct exchange interaction between d shells ($\propto \mathbf{S}^A \cdot \mathbf{S}^B$) is neglected here, that is due to long interionic distance R .

Now let us write the matrix elements of the exchange operator (19) using the following simple basis: $|p, \mu, \lambda, \nu\rangle$, with $p = \pm 1$; $\mu, \lambda, \nu = \pm 1/2$ (here the designations $\mu = s_z$, $\lambda = S_z^A$, $\nu = S_z^B$ are introduced). These elements of the 16×16 matrix are given by

It is convenient to use the triplet/singlet basis $|S, S_z\rangle$ for pair of d -shell spins ($\mathbf{S} = \mathbf{S}^A + \mathbf{S}^B$). This allows us to trace the alignment of d shells in a simpler way. For a triplet state there are $S = 1$ with $S_z = 0, \pm 1$, and for a singlet state $S = 0$, $S_z = 0$. A unitary transformation to this basis is presented in the Appendix C.

Some restrictions are imposed by the axial symmetry of the problem: the z projection of the total angular momentum Σ_z is a good quantum number (in the approximation used, the orbital momentum is zero, so Σ is the sum of the electron spin \mathbf{s} and the total spin $\mathbf{S} = \mathbf{S}^A + \mathbf{S}^B$ of d shells). Using a Σ_z -classified basis set makes the solution of the spectral problem more clear. The transformation corresponding to transition to this basis is presented in Appendix C as well. The matrices of the exchange operator and the complete Hamiltonian are sufficiently simplified in the $|p, S, \Sigma, \Sigma_z\rangle$ basis. In this basis, the Hamiltonian is divided into eight 1×1 blocks and four 2×2 blocks. However, the final matrix 16×16 is not written out here due to its cumbersome form.

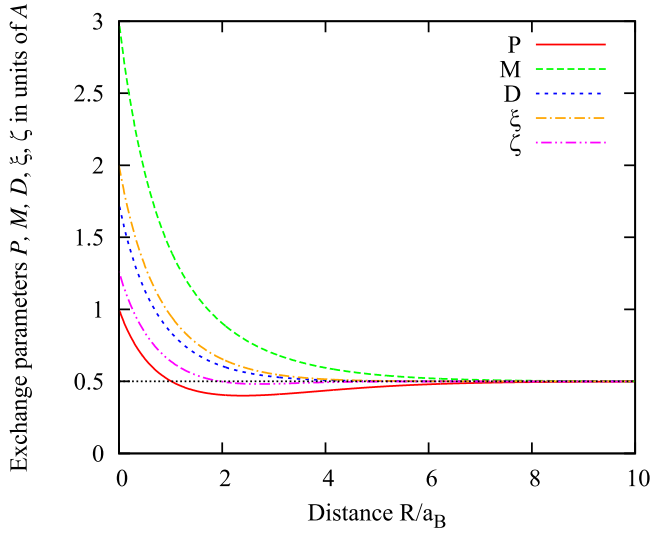


FIG. 2. Dependence of exchange parameters P , M , D , ξ , and ζ on interionic distance R .

The results of the Hamiltonian diagonalization are presented in Table I. The states are divided into two- and fourfold degenerate depending on the value of the total three-particle spin Σ , $1/2$, or $3/2$, respectively. It may seem that there is a contradiction: basis functions with opposite permutation parity p are mixed in states 3–6. However, there is no discrepancy here, since the p parity is a property of the spinless problem, whereas in the problem with spins, the type of the total wave function (symmetric/antisymmetric) also depends on the permutation of the d -shell spins. So, for example, the states $|+, 0, 1/2, +1/2\rangle$ and $|-, 1, 1/2, +1/2\rangle$ are both antisymmetric with respect to the permutation of the ions A and B . This is a consequence of the antisymmetry and symmetry relative to the $A \leftrightarrow B$ permutation of singlet $|0, 0\rangle = \frac{1}{\sqrt{2}}(\uparrow\downarrow - \downarrow\uparrow)$ and triplet $|1, 0\rangle = \frac{1}{\sqrt{2}}(\uparrow\downarrow + \downarrow\uparrow)$ and $|1, +1\rangle = \uparrow\uparrow$ states, respectively. Here the notation $\uparrow\downarrow$ is used for the state $|S_z^A; S_z^B\rangle = |+1/2; -1/2\rangle$, etc.

The dependence of the energy levels of the magnetic D_2^+ complex on the interionic distance R is plotted in Fig. 3 for both signs of the intracenter exchange constant A . One can see a significant dependence of the level structure on the sign of A . In the case of a large interionic distance ($R \rightarrow \infty$), the exchange splitting is equal to its intracenter value $|A|$

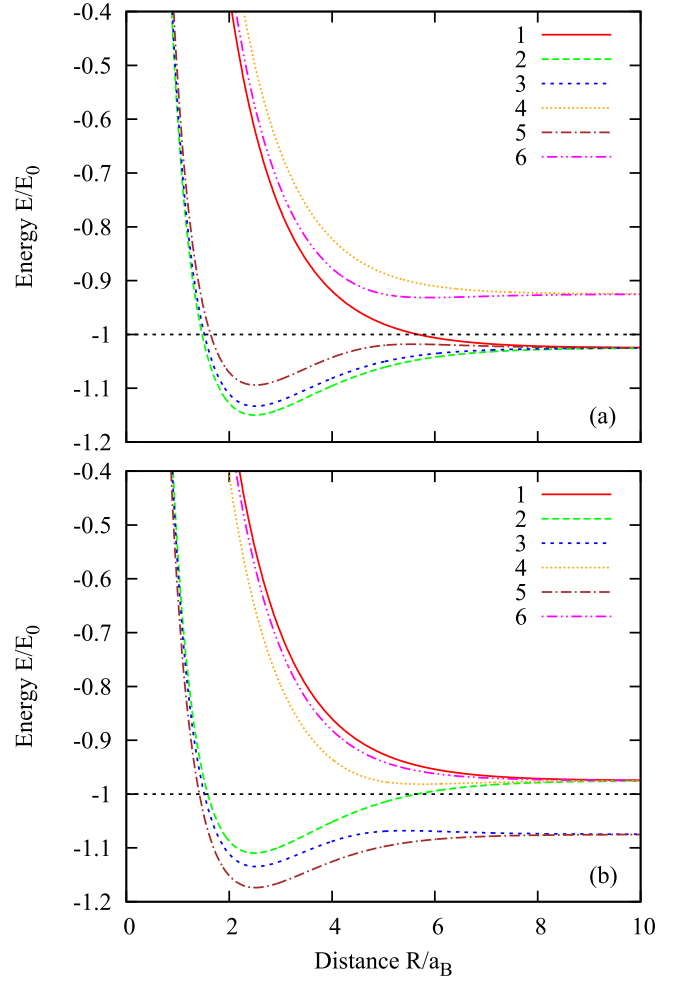


FIG. 3. Dependence of energy levels of magnetic D_2^+ complex on interionic distance R . The curve number corresponds to the number of the energy level E_i in Table I ($i = 1 - 6$). (a) $A = 0.1E_0$ and (b) $A = -0.1E_0$.

that corresponds to the “dissociation” of the D_2^+ complex into the neutral D^0 and ionized D^+ magnetic donors. The levels are split in a ratio of 3:1 relative to the $-E_0$ value [see Eq. (18)]. The degeneracies of these states are $12 = 3 \times 2 \times 2$ and $4 = 1 \times 2 \times 2$ for states split off by energy $\frac{A}{4}$ and $-\frac{3A}{4}$, respectively. In the above products, the first factor

TABLE I. Properties of states of the magnetic D_2^+ complex. Energy levels, wave functions, level degeneracies as well as the d -shell spin expectation values $\langle S^2 \rangle$ and $\langle S_z \rangle$ are presented. The angles η^+ and φ^+ are given by $\tan \eta^+ = \frac{\sqrt{3}D}{E_- - E_+ + M}$ and $\tan \varphi^+ = \frac{\sqrt{3}D}{E_- - E_+ - P}$, respectively.

No.	Deg.	Energy	Wave function	Σ	Σ_z	$\langle S^2 \rangle$	$\langle S_z \rangle$
1	4	$E_- - \frac{M}{2}$	$ -, 1, 3/2, \pm 3/2\rangle, -, 1, 3/2, \pm 1/2\rangle$	$\frac{3}{2}$	$\pm \frac{1}{2}, \pm \frac{3}{2}$	2	$\pm \frac{1}{3}, \pm 1$
2	4	$E_+ - \frac{P}{2}$	$ +, 1, 3/2, \pm 3/2\rangle, +, 1, 3/2, \pm 1/2\rangle$	$\frac{3}{2}$	$\pm \frac{1}{2}, \pm \frac{3}{2}$	2	$\pm \frac{1}{3}, \pm 1$
3	2	$\frac{E_+ + E_- + M}{2} - \sqrt{\left(\frac{E_- - E_+ + M}{2}\right)^2 + \frac{3}{4}D^2}$	$\cos \frac{\eta^+}{2} +, 0, 1/2, \pm 1/2\rangle + \sin \frac{\eta^+}{2} -, 1, 1/2, \pm 1/2\rangle$	$\frac{1}{2}$	$\pm \frac{1}{2}$	$1 - \cos \eta^+$	$\pm \frac{1}{3}(1 - \cos \eta^+)$
4	2	$\frac{E_+ + E_- + M}{2} + \sqrt{\left(\frac{E_- - E_+ + M}{2}\right)^2 + \frac{3}{4}D^2}$	$\sin \frac{\eta^+}{2} +, 0, 1/2, \pm 1/2\rangle - \cos \frac{\eta^+}{2} -, 1, 1/2, \pm 1/2\rangle$	$\frac{1}{2}$	$\pm \frac{1}{2}$	$1 + \cos \eta^+$	$\pm \frac{1}{3}(1 + \cos \eta^+)$
5	2	$\frac{E_+ + E_- + P}{2} - \sqrt{\left(\frac{E_- - E_+ - P}{2}\right)^2 + \frac{3}{4}D^2}$	$\cos \frac{\varphi^+}{2} +, 1, 1/2, \pm 1/2\rangle + \sin \frac{\varphi^+}{2} -, 0, 1/2, \pm 1/2\rangle$	$\frac{1}{2}$	$\pm \frac{1}{2}$	$1 + \cos \varphi^+$	$\pm \frac{1}{3}(1 + \cos \varphi^+)$
6	2	$\frac{E_+ + E_- + P}{2} + \sqrt{\left(\frac{E_- - E_+ - P}{2}\right)^2 + \frac{3}{4}D^2}$	$\sin \frac{\varphi^+}{2} +, 1, 1/2, \pm 1/2\rangle - \cos \frac{\varphi^+}{2} -, 0, 1/2, \pm 1/2\rangle$	$\frac{1}{2}$	$\pm \frac{1}{2}$	$1 - \cos \varphi^+$	$\pm \frac{1}{3}(1 - \cos \varphi^+)$

corresponds to the spin multiplicity of a single magnetic D^0 donor (triplet/singlet). The second one corresponds to two possible configurations: the center A is neutral, the center B is ionized, and vice versa. The third corresponds to two possible orientations of the d -shell spin in the ionized D^+ donor.

B. Magnetic D_2^0 complex

Here, the exchange coupling between both electrons ($i = 1, 2$) and the magnetic shells of both ions ($j = A, B$) of the magnetic complex D_2^0 is taken into account. The corresponding operator has usual isotropic form

$$H_{ex}^{D_2^0} = - \sum_{i=1,2} \sum_{j=A,B} \mathcal{J}(|\mathbf{r}_i - \mathbf{R}_j|) \mathbf{s}^i \cdot \mathbf{S}^j. \quad (22)$$

The direct exchange of the form $\mathbf{S}^A \cdot \mathbf{S}^B$ is not taken into account here, as in the case of the magnetic D_2^+ complex.

The ground (singlet, $|0, 0\rangle$) and first excited (triplet, $|1, 0\rangle$, $|1, \pm 1\rangle$) electron states of the D_2^0 complex are taken into account (total electron spin $\mathbf{s} = \mathbf{s}^1 + \mathbf{s}^2$). The inner magnetic shells of spin $1/2$ are also described in terms of the total spin of two shells ($\mathbf{S} = \mathbf{S}^A + \mathbf{S}^B$). Here, the main and painstaking work is to write the exchange operators $\mathbf{s}^i \cdot \mathbf{S}^j$ ($i = 1, 2$ and $j = A, B$) in double singlet/triplet basis $|s, s_z\rangle \otimes |S, S_z\rangle$. These four 16×16 matrices have cumbersome form and are not presented here. The symmetry of the problem points out that the z projection of the total spin $\Sigma_z = s_z^1 + s_z^2 + S_z^A + S_z^B$ is a good quantum number, i.e., the states of magnetic D_2^0 complex can be classified with respect to Σ_z .

Now it is necessary to find the matrix elements of the exchange coupling strength $\mathcal{J}(|\mathbf{r}_i - \mathbf{R}_j|)$ between the envelopes Φ_k ($k = 1, 2$) multiplied by s -like Bloch functions. The two-particle wave functions Φ_1 and Φ_2 possess a definite parity with respect to permutations of ions $A \leftrightarrow B$, and electrons $1 \leftrightarrow 2$. Because of this symmetry, only the matrix element of $\mathcal{J}(|\mathbf{r}_1 - \mathbf{R}_A|)$ must be found, others can differ only in sign. The matrix element $\langle S\Phi_1 | \mathcal{J}(|\mathbf{r}_1 - \mathbf{R}_A|) | \Phi_1 S \rangle$ is nonzero. However, its form is not written out here, since it is multiplied by the zero 4×4 block in all four matrices $\mathbf{s}^i \cdot \mathbf{S}^j$ (this block comes from the electron singlet state).

Two matrix elements of interest lead us to two new exchange parameters, which can be expressed in terms of the exchange parameters P , M , and D ,

$$\xi(R) = \langle S\Phi_2 | \mathcal{J}(|\mathbf{r}_1 - \mathbf{R}_A|) | \Phi_2 S \rangle = \frac{1}{2} [P(R) + M(R)], \quad (23)$$

$$\zeta(R) = \langle S\Phi_2 | \mathcal{J}(|\mathbf{r}_1 - \mathbf{R}_A|) | \Phi_1 S \rangle = \cos\left(\frac{\theta}{2} - \frac{\pi}{4}\right) D(R). \quad (24)$$

These parameters describe an exchange within the electron triplet states and the mixing of triplet and singlet states, respectively. The dependencies $\xi(R)$ and $\zeta(R)$ are depicted in Fig. 2.

Using the basis set $|s, s_z; S, S_z\rangle$ and above-mentioned matrices $\mathbf{s}^i \cdot \mathbf{S}^j$ ($i = 1, 2$ and $j = A, B$) the following form of the

exchange Hamiltonian (22) is found:

$$H_{ex}^{D_2^0} = \begin{pmatrix} H_{11} & H_{12} & 0 & H_{14} \\ H_{12}^\dagger & 0 & H_{12} & H_{24} \\ 0 & H_{12}^\dagger & -H_{11} & -H_{14}^\dagger \\ H_{14}^\dagger & H_{24}^\dagger & -H_{14} & 0 \end{pmatrix}, \quad (25)$$

which is presented as a composition of 4×4 blocks. Here 0 is the 4×4 zero matrix. The high symmetry of the exchange matrix is a consequence of the time-reversal symmetry. The nonzero blocks are expressed in terms of four 4×4 matrices,

$$H_{11} = -\xi \begin{pmatrix} 1 & 0 & 0 & 0 \\ 0 & 0 & 0 & 0 \\ 0 & 0 & -1 & 0 \\ 0 & 0 & 0 & 0 \end{pmatrix}, \quad H_{12} = -\xi \begin{pmatrix} 0 & 0 & 0 & 0 \\ 1 & 0 & 0 & 0 \\ 0 & 1 & 0 & 0 \\ 0 & 0 & 0 & 0 \end{pmatrix}, \quad (26a)$$

$$H_{14} = -\zeta \begin{pmatrix} 0 & 0 & 0 & 0 \\ 0 & 0 & 0 & 0 \\ 0 & 0 & 0 & -1 \\ 1 & 0 & 0 & 0 \end{pmatrix}, \quad H_{24} = -\zeta \begin{pmatrix} 0 & 0 & 0 & 0 \\ 0 & 0 & 0 & 1 \\ 0 & 0 & 0 & 0 \\ 0 & 1 & 0 & 0 \end{pmatrix}. \quad (26b)$$

The following order of basis functions $|s, s_z; S, S_z\rangle$ is used in Eq. (25): $|1, +1; 1, +1\rangle$, $|1, +1; 1, 0\rangle$, $|1, +1; 1, -1\rangle$, $|1, +1; 0, 0\rangle$, $|1, 0; 1, +1\rangle$, $|1, 0; 1, 0\rangle$, $|1, 0; 1, -1\rangle$, $|1, 0; 0, 0\rangle$, $|1, -1; 1, +1\rangle$, $|1, -1; 1, 0\rangle$, $|1, -1; 1, -1\rangle$, $|1, -1; 0, 0\rangle$, $|0, 0; 1, +1\rangle$, $|0, 0; 1, 0\rangle$, $|0, 0; 1, -1\rangle$, $|0, 0; 0, 0\rangle$.

An exchange-independent part of the Hamiltonian is obviously given by

$$H^{D_2^0} = \begin{pmatrix} E_t I & 0 & 0 & 0 \\ 0 & E_t I & 0 & 0 \\ 0 & 0 & E_t I & 0 \\ 0 & 0 & 0 & E_s I \end{pmatrix}, \quad (27)$$

where I is the 4×4 identity matrix.

Results of the Hamiltonian $H^{D_2^0} + H_{ex}^{D_2^0}$ diagonalization, classification of wave functions as well as expectation values of S^2 and S_z operators for d -shell spins are presented in Table II.

The energy levels of the magnetic D_2^0 complex as a function of the interionic distance R are plotted in Fig. 4 for both signs of the intracenter exchange constant A . In the case of a large interionic distance ($R \rightarrow \infty$), there are three levels with different degeneracies, which are separated from each other by the intracenter value $|A|$. This corresponds to the ‘‘dissociation’’ of the D_2^0 complex into two magnetic D^0 donors. The energy shifts, counted from the nonmagnetic value $-2E_0$, can be found by combination of level shifts of two magnetic D^0 centers from Eq. (18): $-\frac{A}{2} = 2\left(-\frac{A}{4}\right)$, $\frac{A}{2} = -\frac{A}{4} + \frac{3A}{4}$, $\frac{3A}{2} = 2\left(\frac{3A}{4}\right)$. The level degeneracies in the $R \rightarrow \infty$ limit can be found combining two sets of singlets/triplets: $3 \times 3 = 9$, $1 \times 3 \times 2 = 6$, and $1 \times 1 = 1$ correspond to the same order as for energy levels. The factor 2 corresponds to two possible realizations: a singlet at the A center and a triplet at the B center, and vice versa.

TABLE II. Properties of states of the magnetic D_2^0 complex. Energy levels, wave functions, level degeneracies as well as the inner shell spin expectation values $\langle S^2 \rangle$ and $\langle S_z \rangle$ are presented. The angles η^0 and φ^0 are determined by $\tan \eta^0 = \frac{2\xi}{E_t - E_s}$ and $\tan \varphi^0 = \frac{2\sqrt{3}\xi}{E_t - E_s + 2\xi}$, respectively. Here, for the sake of brevity, the following notations are introduced: $|t; 0, 0\rangle = \frac{1}{\sqrt{3}}(|1, +1; 1, -1\rangle - |1, 0; 1, 0\rangle + |1, -1; 1, +1\rangle)$, $|s; 0, 0\rangle = |0, 0; 0, 0\rangle$

No.	Deg.	Energy	Wave function	Σ	Σ_z	$\langle S^2 \rangle$	$\langle S_z \rangle$
1	5	$E_t - \xi$	$ 1, \pm 1; 1, \pm 1\rangle, \frac{1}{\sqrt{2}}(1, \pm 1; 1, 0\rangle + 1, 0; 1, \pm 1\rangle),$ $\frac{1}{\sqrt{6}}(1, +1; 1, -1\rangle + 2 1, 0; 1, 0\rangle + 1, -1; 1, +1\rangle)$	2	$0, \pm 1, \pm 2$	2	$0, \pm \frac{1}{2}, \pm 1$
2	3	$E_t + \xi$	$\frac{1}{\sqrt{2}}(1, \pm 1; 1, 0\rangle - 1, 0; 1, \pm 1\rangle),$ $\frac{1}{\sqrt{2}}(1, +1; 1, -1\rangle - 1, -1; 1, +1\rangle)$	1	$0, \pm 1$	2	$0, \pm \frac{1}{2}$
3	3	$\frac{E_t + E_s}{2} - \sqrt{\left(\frac{E_t - E_s}{2}\right)^2 + \zeta^2}$	$\sin \frac{\eta^0}{2} 1, 0(\pm 1); 0, 0\rangle - \cos \frac{\eta^0}{2} 0, 0; 1, 0(\pm 1)\rangle$	1	$0, \pm 1$	$1 + \cos \eta^0$	$0, \pm \frac{1}{2}(1 + \cos \eta^0)$
4	3	$\frac{E_t + E_s}{2} + \sqrt{\left(\frac{E_t - E_s}{2}\right)^2 + \zeta^2}$	$\cos \frac{\eta^0}{2} 1, 0(\pm 1); 0, 0\rangle + \sin \frac{\eta^0}{2} 0, 0; 1, 0(\pm 1)\rangle$	1	$0, \pm 1$	$1 - \cos \eta^0$	$0, \pm \frac{1}{2}(1 - \cos \eta^0)$
5	1	$\frac{E_t + E_s + 2\xi}{2} - \sqrt{\left(\frac{E_t - E_s + 2\xi}{2}\right)^2 + 3\xi^2}$	$\sin \frac{\varphi^0}{2} t; 0, 0\rangle + \cos \frac{\varphi^0}{2} s; 0, 0\rangle$	0	0	$1 - \cos \varphi^0$	0
6	1	$\frac{E_t + E_s + 2\xi}{2} + \sqrt{\left(\frac{E_t - E_s + 2\xi}{2}\right)^2 + 3\xi^2}$	$\cos \frac{\varphi^0}{2} t; 0, 0\rangle - \sin \frac{\varphi^0}{2} s; 0, 0\rangle$	0	0	$1 + \cos \varphi^0$	0

IV. INDIRECT EXCHANGE INTERACTION

In previous section the level structure of the magnetic D_2^+ and D_2^0 complexes was studied. Let us now discuss the spin structure of these complexes. This will allow us to draw conclusions on the strength of indirect exchange interaction in DMSs in the insulating phase. The dependencies of the total spin of the d shells on the interionic distance R in states of D_2^+ and D_2^0 complexes (see Tables I and II) are depicted in Figs. 5 and 6. It can be seen that the exchange mediated by one electron, as in the D_2^+ complex, corresponds to ferromagnetic (FM) alignment. This is similar, especially at short and intermediate interionic distances R , to the so-called double exchange (see, for instance, Ref. [38]). The exchange alignment mediated by two charge carriers, as in the D_2^0 complex, at short R looks like antiferromagnetic (AFM) superexchange [38].

At short interionic distance R the d -shell alignment for both complexes can be explained in classical manner. In this case the d shells have FM and AFM alignment for D_2^+ and D_2^0 complex, respectively, regardless of the sign of the intracenter parameter A . In the case of the D_2^+ complex, both d -shell spins are aligned either parallel or antiparallel to the electron spin, i.e., they have FM alignment relative to each other. In ground state of D_2^0 complex (spin singlet), depending on the sign of parameter A , there are either $\uparrow\uparrow\downarrow\downarrow$ or $\downarrow\uparrow\downarrow\uparrow$ configurations, both corresponding to AFM d -shell alignment (the electron and d -shell spins are denoted by thin and thick arrows, respectively). As the interionic distance R increases, the mixing of excited electronic states occurs, and the d -shell spin orientation deviates from strong FM and AFM alignment corresponding to double exchange and superexchange, respectively.

The spectral problem for the magnetic D_2^0 complex can be solved by means of the perturbation theory. The same result can be obtained simply by expanding the exact result (Table II) with respect to the small parameter $|A|/(E_t - E_s) \ll 1$. The last condition is satisfied when the interionic distances are not too large. The perturbative approach allows to trace the proximity of the E_3 and E_5 levels (both levels originate from

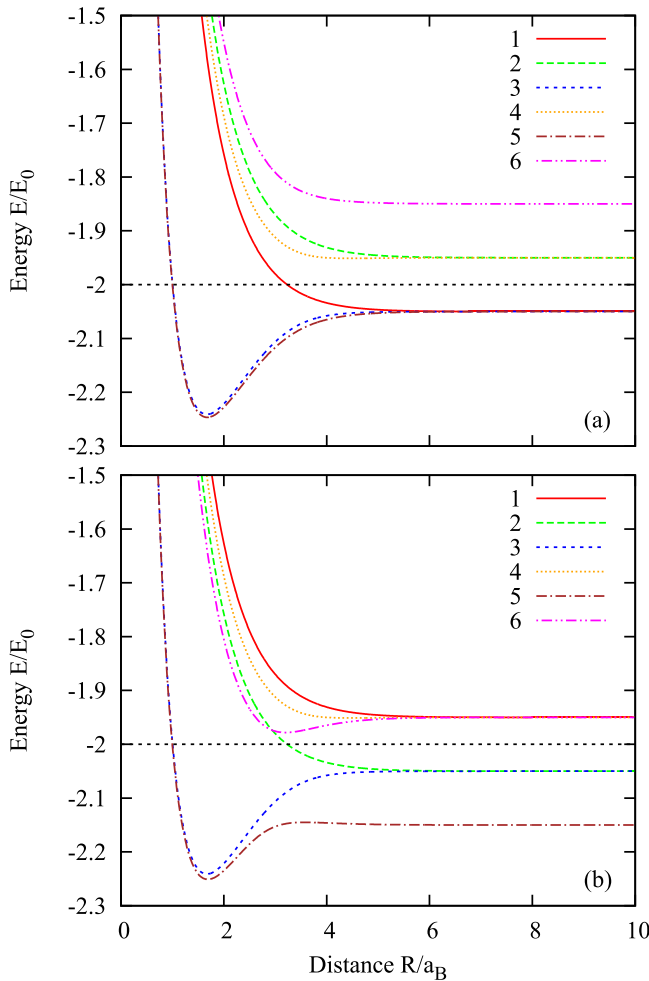


FIG. 4. Dependence of energy levels of magnetic D_2^0 complex on interionic distance R . The curve number corresponds to the number of the energy level E_i in Table II ($i = 1 - 6$). (a) $A = 0.1E_0$ and (b) $A = -0.1E_0$.

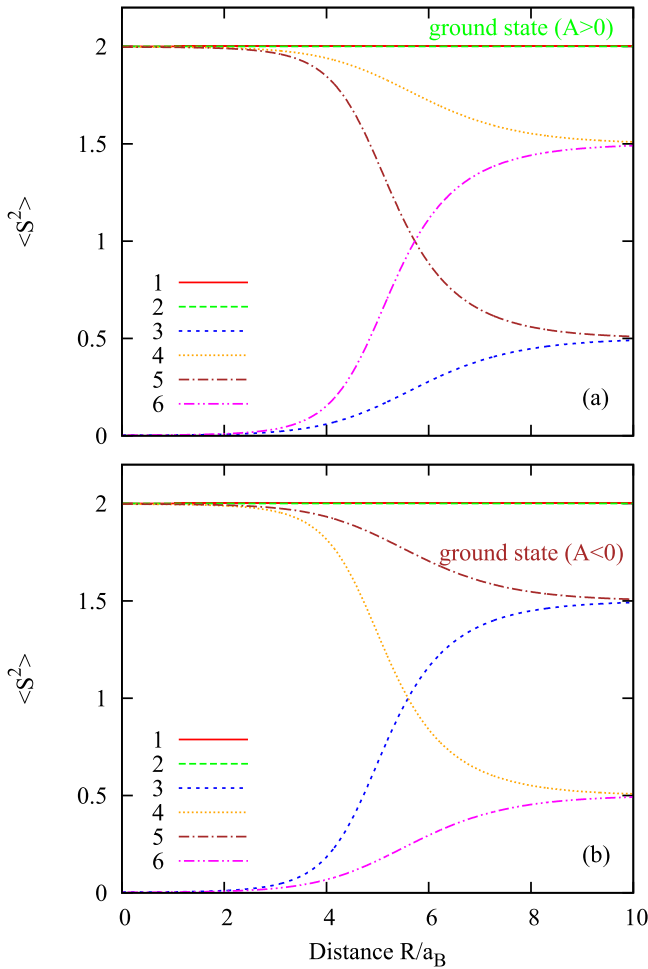


FIG. 5. Dependence of the squared spin expectation value of a pair of d shells in states of the D_2^+ complex with energies E_i ($i = 1 - 6$) on interionic distance R . The curve number corresponds to the number of the energy level in Table I. (a) $A = 0.1E_0$ and (b) $A = -0.1E_0$.

electronic singlet state),

$$E_3 = E_s - \frac{\zeta^2}{E_t - E_s}, \quad E_5 = E_s - \frac{3\zeta^2}{E_t - E_s}. \quad (28)$$

The energies E_3 and E_5 do not depend on the sign of exchange parameter A in approximation used. This is fulfilled for distances R up to $\sim 2.5a_B$ for the case of $|A| = 0.1E_0$ (see Fig. 4). If perturbation theory is applicable, then our results for the complexes D_2^+ and D_2^0 can be obtained by methods usual in the theory of indirect exchange, i.e., considering configurations of d shells parametrically (see Appendix D). The dependence on the sign of A appears for large R and can be traced using the following order of perturbation theory.

The opposite limit of large interionic distance ($R \gg 1$) is also of interest. In this case, it is convenient to use single-center states as a basis. The wave function of D_2^+ complex at $R \rightarrow \infty$ is a combination of the wave functions of the noninteracting neutral magnetic D^0 and ionized magnetic D^+ donors located at \mathbf{R}_A and \mathbf{R}_B , and vice versa. The corresponding states are described by single-center triplet/singlet eigenvectors $|S, S_z\rangle_{A(B)}$ and d -shell eigenvectors $|\pm 1/2\rangle_{A(B)}$,

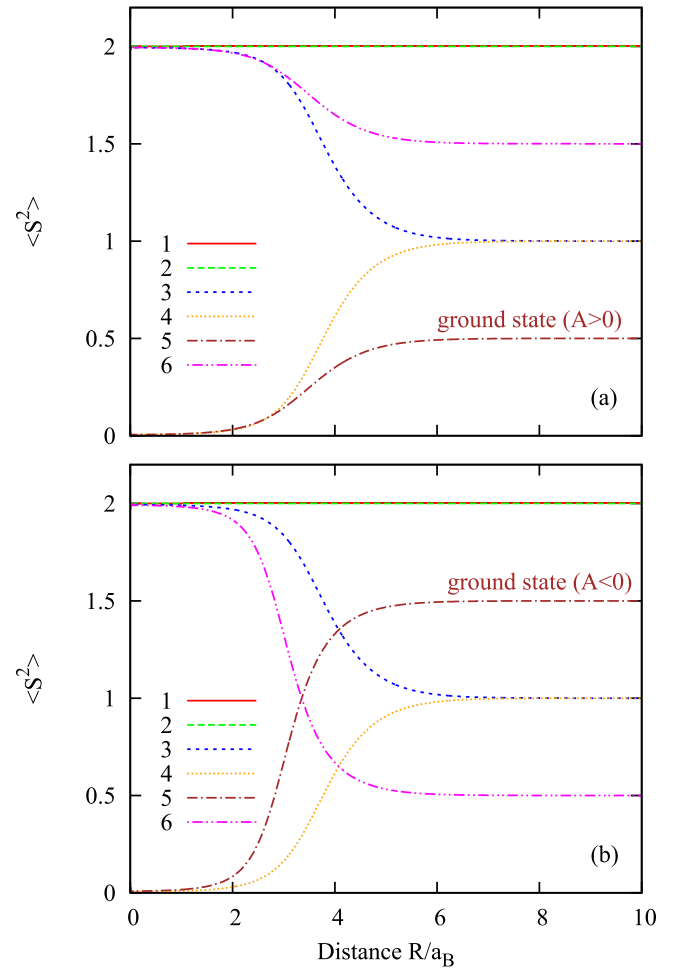


FIG. 6. Dependence of the squared spin expectation value of a pair of d shells in state of the D_2^0 complex with energy E_i ($i = 1 - 6$) on interionic distance R . The curve number corresponds to the number of the energy level in Table II. (a) $A = 0.1E_0$ and (b) $A = -0.1E_0$.

respectively. The magnetic D_2^0 complex in the above limit is a combination of two neutral magnetic D^0 donors. The results for the magnetic D_2^+ and D_2^0 complexes corresponding to the limit $R \rightarrow \infty$ are summarized in Table III and IV, respectively.

It should be noted that the discussed problem of the magnetic D_2^+ and D_2^0 complexes resembles the problem of hydrogen molecule ion H_2^+ and hydrogen molecule H_2 , respectively, taking into account the Fermi contact part (δ -like) of the hyperfine interaction. This is the consequence of the EFA decomposition and short-range behavior of the intracenter exchange strength $\mathcal{J}(r)$. However, there are significant differences. Firstly, this is the presence of a rotational (spatial) wave function in para- and ortho-hydrogen, which, in accordance with the fact that protons are fermions (spin of $1/2$), should have opposite parity, and therefore different orbital angular momentum, for para- and ortho-hydrogen, respectively. The rotational splitting is much larger than the splitting due to the hyperfine interaction. Secondly, there is a significant difference in the strength of interaction in impurity complexes and atomic (or molecular) systems. The characteristic en-

TABLE III. Properties of states of the magnetic D_2^+ complex in the $R \rightarrow \infty$ limit. Energy levels, wave functions, level degeneracies as well as the d -shell spin expectation values $\langle S^2 \rangle$ and $\langle S_z \rangle$ are presented. Eigenstates are presented as a combination of single-center eigenstates of the A (B) center, which can be occupied by an electron (electron spin + d -shell spin, singlet/triplet) or simply ionized (d -shell spin of $1/2$ only with possible $\pm 1/2$ projections). The case $A > 0$ is considered. In the opposite case ($A < 0$) the energies are the same but the eigenstates (and consequently spin properties such $\langle S^2 \rangle$) for levels 3 and 4, as well as for 5 and 6 should be interchanged.

No.	Deg.	Energy	Wave function	Σ	Σ_z	$\langle S^2 \rangle$	$\langle S_z \rangle$
1	4	$-E_0 - \frac{A}{4}$	$\frac{1}{\sqrt{2}}(1, \pm 1\rangle_A \pm 1/2\rangle_B - \pm 1/2\rangle_A 1, \pm 1\rangle_B),$ $\frac{1}{\sqrt{6}}(1, \pm 1\rangle_A \mp 1/2\rangle_B - \mp 1/2\rangle_A 1, \pm 1\rangle_B) + \frac{1}{\sqrt{3}}(1, 0\rangle_A \pm 1/2\rangle_B - \pm 1/2\rangle_A 1, 0\rangle_B)$	$\frac{3}{2}$	$\pm \frac{1}{2}, \pm \frac{3}{2}$	2	$\pm \frac{1}{3}, \pm 1$
2	4	$-E_0 - \frac{A}{4}$	$\frac{1}{\sqrt{2}}(1, \pm 1\rangle_A \pm 1/2\rangle_B + \pm 1/2\rangle_A 1, \pm 1\rangle_B),$ $\frac{1}{\sqrt{6}}(1, \pm 1\rangle_A \mp 1/2\rangle_B + \mp 1/2\rangle_A 1, \pm 1\rangle_B) + \frac{1}{\sqrt{3}}(1, 0\rangle_A \pm 1/2\rangle_B + \pm 1/2\rangle_A 1, 0\rangle_B)$	$\frac{3}{2}$	$\pm \frac{1}{2}, \pm \frac{3}{2}$	2	$\pm \frac{1}{3}, \pm 1$
3	2	$-E_0 - \frac{A}{4}$	$\frac{1}{\sqrt{3}}(1, \pm 1\rangle_A \mp 1/2\rangle_B - \mp 1/2\rangle_A 1, \pm 1\rangle_B) - \frac{1}{\sqrt{6}}(1, 0\rangle_A \pm 1/2\rangle_B - \pm 1/2\rangle_A 1, 0\rangle_B)$	$\frac{1}{2}$	$\pm \frac{1}{2}$	$\frac{1}{2}$	$\pm \frac{1}{6}$
4	2	$-E_0 + \frac{3A}{4}$	$\frac{1}{\sqrt{2}}(0, 0\rangle_A \pm 1/2\rangle_B - \pm 1/2\rangle_A 0, 0\rangle_B)$	$\frac{1}{2}$	$\pm \frac{1}{2}$	$\frac{3}{2}$	$\pm \frac{1}{2}$
5	2	$-E_0 - \frac{A}{4}$	$\frac{1}{\sqrt{3}}(1, \pm 1\rangle_A \mp 1/2\rangle_B + \mp 1/2\rangle_A 1, \pm 1\rangle_B) - \frac{1}{\sqrt{6}}(1, 0\rangle_A \pm 1/2\rangle_B + \pm 1/2\rangle_A 1, 0\rangle_B)$	$\frac{1}{2}$	$\pm \frac{1}{2}$	$\frac{1}{2}$	$\pm \frac{1}{6}$
6	2	$-E_0 + \frac{3A}{4}$	$\frac{1}{\sqrt{2}}(0, 0\rangle_A \pm 1/2\rangle_B + \pm 1/2\rangle_A 0, 0\rangle_B)$	$\frac{1}{2}$	$\pm \frac{1}{2}$	$\frac{3}{2}$	$\pm \frac{1}{2}$

ergy scale of the exchange interaction is determined by the intracenter exchange parameter A , which has a typical scale of up to $|A|/E_0 \sim 0.1$. The relative magnitude of hyperfine splitting in the hydrogen atom is given by [39]

$$\frac{\Delta E_{hf}}{\text{Ry}} = \frac{8}{3} \alpha^2 \frac{m_e}{m_p} g_p,$$

where $\alpha = \frac{e^2}{\hbar c} \simeq \frac{1}{137}$ is the fine structure constant, m_e is the free electron mass, $m_p = 1836m_e$ and $g_p \simeq 5.59$ are proton mass and g-factor, respectively. Thus, the relative magnitude of hyperfine splitting is approximately equal to 4.3×10^{-7} . The hyperfine splitting of the ground state of the H_2 molecule is usually assumed to be zero, since there are two electrons with opposite spins. However, by analogy with our perturbative consideration (28), the hyperfine splitting of the ground state of the H_2 molecule is estimated to be approximately 10^{-13} eV. This splitting is negligible compared to the rotational one, 118 cm^{-1} (about 1.46×10^{-2} eV). Apparently, the weakness of the hyperfine interaction allows to retain “para/ortho” nomenclature. The third difference is the possibility of realizing both signs of the exchange parameter A , while the hyperfine interaction strength has a fixed sign and is simply proportional to the product of the magnetic moments of the proton and electron.

So far, we have solved only problems about the level and spin structure of two-center magnetic complexes. These results do not really answer the question “what magnetic order will be in a system?”. However, our results can be used to determine the type of magnetic ordering and estimate the Curie temperature. To do this, the simulation in the spirit of the so-called disordered Heisenberg model can be used. It is necessary to take into account two types of disorder: (i) disorder associated with the spread in the interionic distance; (ii) disorder corresponding to the simultaneous realization of two mechanisms of indirect exchange with opposite (FM and AFM) alignment. Similar calculations were recently performed in the simpler case of the disordered Ising model [40–42]. Our result can also be used in the mean-field [25,26] or Monte Carlo [27,28] simulations. The results of above studies [25–28] should be revisited, since the compensation due to Mn interstitials that now is accepted to be responsible for compensation in GaMnAs was not taken into account.

The simple estimates are possible in some limiting cases. In the case of compensation close to zero, there is approximately one hole per one manganese atom. In this case, the pair interaction corresponds to the AFM alignment, as in the magnetic D_2^0 complex. However, a strong AFM order should not be expected. This is a consequence of two reasons: (i)

TABLE IV. Properties of states of the magnetic D_2^0 complex in the $R \rightarrow \infty$ limit. Energy levels, wave functions, level degeneracies as well as the d -shell spin expectation values $\langle S^2 \rangle$ and $\langle S_z \rangle$ are presented. Eigenstates are presented as a combination of single-center (electron spin + d -shell spin, singlet/triplet) eigenstates. The case $A > 0$ is considered. In the opposite case ($A < 0$), the energies can be found from Table II, while the eigenstates for levels 3 and 4, as well as for 5 and 6 should be interchanged.

No.	Deg.	Energy	Wave function	Σ	Σ_z	$\langle S^2 \rangle$	$\langle S_z \rangle$
1	5	$-2E_0 - \frac{A}{2}$	$ 1, \pm 1\rangle_A 1, \pm 1\rangle_B, \frac{1}{\sqrt{2}}(1, \pm 1\rangle_A 1, 0\rangle_B - 1, 0\rangle_A 1, \pm 1\rangle_B),$ $\frac{1}{\sqrt{6}}(1, +1\rangle_A 1, -1\rangle_B + 2 1, 0\rangle_A 1, 0\rangle_B + 1, -1\rangle_A 1, +1\rangle_B)$	2	$0, \pm 1, \pm 2$	2	$0, \pm \frac{1}{2}, \pm 1$
2	3	$-2E_0 + \frac{A}{2}$	$\frac{1}{\sqrt{2}}(1, 0(\pm 1)\rangle_A 0, 0\rangle_B + 0, 0\rangle_A 1, 0(\pm 1)\rangle_B)$	1	$0, \pm 1$	2	$0, \pm \frac{1}{2}$
3	3	$-2E_0 - \frac{A}{2}$	$\frac{1}{\sqrt{2}}(1, 0(\pm 1)\rangle_A 0, 0\rangle_B - 0, 0\rangle_A 1, 0(\pm 1)\rangle_B)$	1	$0, \pm 1$	1	$0, \pm \frac{1}{2}$
4	3	$-2E_0 + \frac{A}{2}$	$\frac{1}{\sqrt{2}}(1, +1\rangle_A 1, -1\rangle_B - 1, -1\rangle_A 1, +1\rangle_B), \frac{1}{\sqrt{2}}(1, \pm 1\rangle_A 1, 0\rangle_B - 1, 0\rangle_A 1, \pm 1\rangle_B)$	1	$0, \pm 1$	1	$0, \pm \frac{1}{2}$
5	1	$-2E_0 - \frac{A}{2}$	$\frac{1}{2\sqrt{3}}(3 0, 0\rangle_A 0, 0\rangle_B - 1, 0\rangle_A 1, 0\rangle_B + 1, +1\rangle_A 1, -1\rangle_B + 1, -1\rangle_A 1, +1\rangle_B)$	0	0	$\frac{1}{2}$	0
6	1	$-2E_0 + \frac{3A}{2}$	$\frac{1}{2}(1, 0\rangle_A 1, 0\rangle_B + 0, 0\rangle_A 0, 0\rangle_B - 1, +1\rangle_A 1, -1\rangle_B - 1, -1\rangle_A 1, +1\rangle_B)$	0	0	$\frac{3}{2}$	0

the possibility of thermal excitation of the FM pair alignment (the first excited state of the magnetic D_2^0 complex has the opposite spin structure of the d shells); (ii) the spread in the interionic distance R . Perhaps a spin glass-like structure can be realized at zero compensation. In the opposite case of complete compensation, the disappearance of magnetic order is also expected, which is due to the absence of charge carriers mediating indirect exchange. The most interesting is the case of intermediate compensation, when the numbers of ionized (Mn_{Ga}^-) and neutral (Mn_{Ga}^0) centers are approximately equal [43]. In this case, there is only one mechanism of indirect exchange: the pair alignment of d shells is mediated by a single charge carrier, as in the magnetic D_2^+ complex, and the FM ordering is expected. Thus, a necessary condition for ferromagnetism in insulating GaMnAs is not only a high content of the magnetic component, but also a compensation degree that provides approximately equal concentration of neutral and ionized substitutional Mn acceptors. It should be noted that the doping by nonmagnetic donors is more suitable, since the required ratio between the concentrations of ionized and neutral acceptors is achieved at a higher Mn_{Ga} concentration [44]. The above picture of compensation-dependent ferromagnetism is in good agreement with considerations based on the impurity band [45,46], when the ferromagnetism is realized at the Fermi level being close to the middle of the impurity band. Similar conclusions regarding the effect of compensation were made in Ref. [47] based on other considerations.

At the same total manganese concentration, the most pronounced ferromagnetism and a higher Curie temperature should be expected at half compensation. In this case, the only one mechanism of indirect exchange interaction takes place that allows to make a simple mean-field estimation of the Curie temperature [48],

$$k_B T_C = \frac{1}{3} S(S+1) J(\bar{R}). \quad (29)$$

Here $J(R)$ is the parameter of indirect exchange interaction as a function of interionic distance R , k_B is the Boltzmann constant, and the d -shell spin $S = 5/2$ is used for Mn acceptor. An average interionic distance \bar{R} between Mn ions can be estimated from Mn concentration n or atomic content x by means of $\frac{4}{3}\pi\bar{R}^3 n = 1$ and $n = \frac{4x}{a_0^3}$, where a_0 is the lattice constant. For $x \ll 1$ the low-temperature value of the GaAs lattice constant $a_0 = 5.64 \text{ \AA}$ [49] can be used for estimates.

The dependence $J(R)$ can be found from the following equation:

$$J = E_{gs}(\uparrow\downarrow) - E_{gs}(\uparrow\uparrow), \quad (30)$$

where $E_{gs}(\uparrow\uparrow)$ and $E_{gs}(\uparrow\downarrow)$ are the ground-state energies of a two-center complex with parallel and antiparallel spins of d shells, respectively. For the case of exchange mediated by single charge carrier, these energies are given by Eq. (D2) of Appendix D. The dependence $J(R)$, calculated using Eqs. (30) and (D2) is depicted in Fig. 7. The curves are plotted for different values $|A|/E_0$ in the range from 0.01 to 0.1 with an increment of 0.01. In the range of interionic distances $R \leq (2-3)a_B$, corresponding to the Mn concentration of interest,

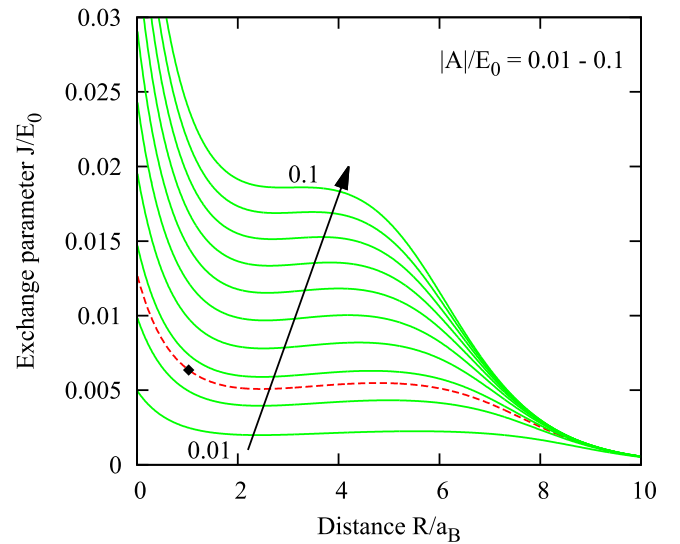


FIG. 7. Dependence of exchange parameter J on interionic distance R for the case of exchange interaction mediated by single charge carrier. The solid-green curves are plotted for the $|A|/E_0$ ratio in (0.01;0.1) interval with 0.01 increment. The dashed-red curve corresponds to parameters of the Mn_{Ga}^0 acceptor in GaAs: $|A|/E_0 = 0.026$. The dot marks the average interionic distance $R = 1.026a_B$ corresponding to the Mn composition $x = 0.01$. The corresponding exchange parameter is equal to $J = 6.35 \times 10^{-3} E_0$.

the strength of indirect exchange interaction can be represented analytically, $J(R) = \frac{1}{2}|P(R)|$. This result corresponds to the first-order perturbation theory in $|A|/(E_- - E_+)$.

There is different information in the literature [50–52] about the magnitude of the exchange parameter A for the Mn_{Ga}^0 acceptor in GaAs: the range 1.2–6 meV is covered in above references. A value of about 2.5 meV [53], obtained using spin-flip Raman spectroscopy, now seems correct. The Mn_{Ga}^0 ionization energy is approximately 110 meV. The value used is $E_0 = 96.9$ meV, which is obtained by subtracting the exchange-dependent part $21|A|/4$ from 110 meV (see, for instance, Ref. [54]). Thus, for the Mn acceptor in GaAs the dimensionless parameter $|A|/E_0 = 0.026$ is used. The corresponding $J(R)$ dependence is depicted in Fig. 7 with a dashed-red curve.

Now let us estimate the Curie temperature T_C at “half-compensation”, which is the upper limit for the fixed Mn content x . The value $x = 0.01$ is used, corresponding to concentration $n = 2.21 \times 10^{20} \text{ cm}^{-3}$ and average intercenter distance $\bar{R} = 1.026a_B$, with Bohr radius of $a_B = 1 \text{ nm}$ [54] for Mn_{Ga}^0 . The value $\bar{R} = 1.026a_B$ is marked with a dot on the corresponding curve in Fig. 7. This point corresponds to the exchange parameter $6.35 \times 10^{-3} E_0$ or 0.615 meV in absolute units. The last value, together with the d -shell spin $S = 5/2$, after substitution into Eq. (29) leads to the Curie temperature about 42 K. Here, the simultaneous use of spin-5/2 in Eq. (29) and spin-1/2 in the definition of the exchange parameter (30) may alert the reader. Let us clarify this issue. The definition of the indirect exchange parameter itself is highly arbitrary. For the case of spin-1/2 there is no other possibility other than Eq. (30). In the case of higher spins, there are more than two configurations. The exchange strength can be defined

as the difference between the ground-state energies for any fixed configuration and the lowest ground-state energy (in our case this is the FM configuration). The Hamiltonian (D1) corresponds to the case of an arbitrary d -shell spin S . The definition of the exchange strength as the difference between the ground-state energies of the spin configurations $(+S; -S)$ and $(+S; +S)$ is proportional to S . At the same time, the difference $E_{gs}(S, S-1) - E_{gs}(S, S)$ is S independent, at least in the range of R values of interest. It is suitable for any S , including $5/2$, and for the case of spin- $1/2$ it coincides with Eq. (30). For small R , the indirect exchange strength determined in this way is equal to $\frac{1}{2}|P(R)|$ regardless of S . For this reason, the simplest definition (30) is used, while the real spin of the Mn d shell ($S = 5/2$) is included in Eq. (29) to determine the Curie temperature of GaMnAs.

Above estimate is in qualitative agreement with experimental data [12], where the value $T_C = 25$ K was measured for a sample with $x = 0.005$. It should be remembered that the mean-field approximation overestimates the value of the critical temperature [28]. The above estimate corresponds to the case when there are no Mn interstitials, and half-compensation is provided by nonmagnetic donors. In the case of half-compensation due to Mn interstitials the x value should be replaced by an effective value $x/2$ [55].

Above estimation should be taken as a qualitative result. This is a consequence of some simplifications of our model. The following features were not taken into account in our consideration: (i) the complex structure of the valence band and acceptor [29,30]; (ii) the short-range part of attracting potential [56] (central-cell correction [54]); (iii) the real value ($5/2$) of the d -shell spin. A real model of the Mn_2^- complex, reflecting the FM type of pair alignment of d shells, can be developed based on the results of Ref. [20] for the nonmagnetic A_2^- complex and Sec. III of present paper.

V. CONCLUSIONS AND OUTLOOK

The energy and spin structure of magnetic D_2^+ and D_2^0 complexes is examined in detail. The indirect exchange interaction in DMS in the insulating phase is studied. It is shown that indirect exchange mediated by one and two charge carriers looks like double- and superexchange, respectively. The competition between the mentioned mechanisms of indirect exchange, and as a consequence, the type of ordering realized in the system is determined primarily by the degree of compensation.

Our results concerning the energy and spin structure of magnetic D_2^+ and D_2^0 complexes do not provide a direct answer to the question of what type of magnetic ordering is realized in real compensated DMSs. However, we believe that these results can be used in various many-body simulations based on the disordered Heisenberg model and the Monte Carlo method.

The simple conclusions are drawn about magnetic ordering for the low, high, and half compensation cases, which are in good agreement with previous theoretical and experimental results. There is no FM ordering at low and high compensation. The particular case of half-compensation (one hole is shared by two Mn acceptors) is of interest. For a fixed total amount of magnetic component, the most pronounced FM

ordering and the highest Curie temperature should be expected at this degree of compensation. An estimate of the Curie temperature of about 40 K for $Ga_{1-x}Mn_xAs$ with $x = 0.01$ is obtained.

The results obtained point out the direction and sequence of actions for studying more realistic complexes Mn_2^- and Mn_2^0 . The complex structure of the valence band significantly modifies and complicates the problem. To calculate the indirect alignment of manganese d shells in GaMnAs, the results for nonmagnetic A_2^- [20] and A_2^0 [57] complexes should be used as a starting point. The second step is to introduce the intracenter exchange interaction for the hole(s) of the complex with real d -shell spins in the same way as in the Sec. III.

ACKNOWLEDGMENTS

We acknowledge financial support from the Russian Science Foundation (Grant No. 22-12-00139). The authors are grateful to I. V. Krainov, I. V. Rozhansky, and V. L. Korenev for useful discussions.

APPENDIX A: INTEGRALS OF D_2^+ PROBLEM

It is convenient to use ellipsoidal coordinates for calculation of overlap integral S , Coulomb integral j' , and resonance integral k' (see, for instance, Ref. [21]),

$$S(a, R) = e^{-aR} \left[1 + aR + \frac{1}{3}(aR)^2 \right], \quad (A1)$$

$$j'(a, R) = \frac{2}{R} [1 - (1 + aR)e^{-2aR}], \quad (A2)$$

$$k'(a, R) = 2a(1 + aR)e^{-aR}. \quad (A3)$$

Here the dependence of integrals on variational parameter a is preserved.

APPENDIX B: INTEGRALS OF D_2^0 PROBLEM

All matrix elements and energies of the H_2 -molecule spectral problem (MO-LCAO approximation) are expressed in terms of E_{\pm} energies and four integrals. Here, for the sake of brevity, the following notation is used: $a(i) = \phi(r_{iA})$, $b(i) = \phi(r_{iB})$ ($i = 1, 2$). A detailed calculation of the integrals used can be found in Slater's book [32].

The single-center integral is given by

$$m = [aa|aa] = \int d\tau_1 d\tau_2 a^2(1)a^2(2) \frac{2}{r_{12}} = \frac{5s}{4R}. \quad (B1)$$

Here the notation $s = aR$ is used.

The two-electron Coulomb integral, which describes the interaction of two electron densities localized at different centers (A and B), has the form

$$j = [aa|bb] = \int d\tau_1 d\tau_2 a^2(1)b^2(2) \frac{2}{r_{12}} = \frac{2}{R} - \frac{1}{R} \left(2 + \frac{11}{4}s + \frac{3}{2}s^2 + \frac{1}{3}s^3 \right) e^{-2s}, \quad (B2)$$

The hybrid integral corresponding to the interaction of the electron density localized at one center with the so-called mixed density has the form

$$l = [aa|ab] = \int d\tau_1 d\tau_2 a^2(1)a(2)b(2) \frac{2}{r_{12}} = \frac{1}{R} \left[\left(\frac{5}{8} + \frac{1}{4}s + 2s^2 \right) e^{-s} - \left(\frac{5}{8} + \frac{1}{4}s \right) e^{-3s} \right]. \quad (\text{B3})$$

The exchange integral is given by

$$k = [ab|ab] = \int d\tau_1 d\tau_2 a(1)b(1)a(2)b(2) \frac{2}{r_{12}} = \frac{2s[A(s) - B(s)]}{5R}, \quad (\text{B4})$$

where

$$\begin{aligned} A(s) &= \frac{6}{s} [(\gamma + \ln s)S^2 - E_1(4s)S^2 + 2E_1(2s)SS'], \\ B(s) &= \left(-\frac{25}{8} + \frac{23}{4}s + 3s^2 + \frac{1}{3}s^3 \right) e^{-2s}, \\ S'(s) &= S(-s) = \left(1 - s + \frac{1}{3}s^2 \right) e^s. \end{aligned}$$

Here $\gamma = 0.57722\dots$ is the Euler-Mascheroni constant, $E_1(x) = \int_x^\infty dz \frac{e^{-z}}{z}$ is the exponential integral [58].

APPENDIX C: BASIS TRANSFORMATIONS

It is convenient to work with a basis that is classified by the total spin S of the d -shell pair and the corresponding projection S_z . The following unitary transformation is required between the old basis $|S_z^A, S_z^B\rangle$ and the new basis $|S, S_z\rangle$:

$$\begin{pmatrix} |1, +1\rangle \\ |1, 0\rangle \\ |1, -1\rangle \\ |0, 0\rangle \end{pmatrix} = \begin{pmatrix} 1 & 0 & 0 & 0 \\ 0 & \frac{1}{\sqrt{2}} & \frac{1}{\sqrt{2}} & 0 \\ 0 & 0 & 0 & 1 \\ 0 & \frac{1}{\sqrt{2}} & -\frac{1}{\sqrt{2}} & 0 \end{pmatrix} \begin{pmatrix} |+\frac{1}{2}, +\frac{1}{2}\rangle \\ |+\frac{1}{2}, -\frac{1}{2}\rangle \\ |-\frac{1}{2}, +\frac{1}{2}\rangle \\ |-\frac{1}{2}, -\frac{1}{2}\rangle \end{pmatrix}. \quad (\text{C1})$$

Due to the axial symmetry of the problem, it is useful to use a basis classified by the total spin of the three particles Σ and its projection Σ_z . The transformation between the basis $|S, \Sigma, \Sigma_z\rangle$ and $|s_z, S, S_z\rangle$ is given by

$$\begin{pmatrix} |0, 1/2, +1/2\rangle \\ |0, 1/2, -1/2\rangle \\ |1, 3/2, +3/2\rangle \\ |1, 3/2, +1/2\rangle \\ |1, 3/2, -1/2\rangle \\ |1, 3/2, -3/2\rangle \\ |1, 1/2, +1/2\rangle \\ |1, 1/2, -1/2\rangle \end{pmatrix} = \begin{pmatrix} 0 & 0 & 0 & 1 & 0 & 0 & 0 & 0 \\ 0 & 0 & 0 & 0 & 0 & 0 & 0 & 1 \\ 1 & 0 & 0 & 0 & 0 & 0 & 0 & 0 \\ 0 & \sqrt{\frac{2}{3}} & 0 & 0 & \frac{1}{\sqrt{3}} & 0 & 0 & 0 \\ 0 & 0 & \frac{1}{\sqrt{3}} & 0 & 0 & \sqrt{\frac{2}{3}} & 0 & 0 \\ 0 & 0 & 0 & 0 & 0 & 0 & 1 & 0 \\ 0 & \frac{1}{\sqrt{3}} & 0 & 0 & -\sqrt{\frac{2}{3}} & 0 & 0 & 0 \\ 0 & 0 & \sqrt{\frac{2}{3}} & 0 & 0 & -\frac{1}{\sqrt{3}} & 0 & 0 \end{pmatrix} \begin{pmatrix} |\uparrow, 1, +1\rangle \\ |\uparrow, 1, 0\rangle \\ |\uparrow, 1, -1\rangle \\ |\uparrow, 0, 0\rangle \\ |\downarrow, 1, +1\rangle \\ |\downarrow, 1, 0\rangle \\ |\downarrow, 1, -1\rangle \\ |\downarrow, 0, 0\rangle \end{pmatrix}. \quad (\text{C2})$$

Here, the quantum number $S = 0, 1$ is additionally used to distinguish two types of states with $\Sigma = 1/2$.

APPENDIX D: MODELS WITH FIXED SPIN CONFIGURATIONS

Now let us consider the models in the usual for exchange interaction manner. In this case, the spin configurations of d shells are assumed to be fixed: the spins are collinear, and possible configurations correspond to parallel ($\uparrow\uparrow$) or antiparallel ($\uparrow\downarrow$)

alignment. In this case the direct (intracenter) exchange is not of Heisenberg-like form [see Eq. (15)], but rather Ising-like, when only z components $s_z^i s_z^j$ are in the dot products of Eqs. (19) and (22). In this case the spectral problems are simplified: the d -shell spins enter the problems as parameters, and there are the 4×4 spectral problems instead of 16×16 ones.

1. Magnetic D_2^+ complex

Since d shells enter the spectral problem as parameters S_z^A and S_z^B , the four basis functions $|p, s_z\rangle$ are used ($p = \pm, s_z = \pm 1/2$). The following order of basis functions $|+, +1/2\rangle, |+, -1/2\rangle, |-, +1/2\rangle$, and $|-, -1/2\rangle$ is utilized. In this case the Hamiltonian of magnetic D_2^+ complex is given by

$$H^{D_2^+}(S_z^A, S_z^B) = \begin{pmatrix} E_+ - \frac{1}{2}P(S_z^A + S_z^B) & 0 & -\frac{1}{2}D(S_z^A - S_z^B) & 0 \\ 0 & E_+ + \frac{1}{2}P(S_z^A + S_z^B) & 0 & \frac{1}{2}D(S_z^A - S_z^B) \\ -\frac{1}{2}D(S_z^A - S_z^B) & 0 & E_- - \frac{1}{2}M(S_z^A + S_z^B) & 0 \\ 0 & \frac{1}{2}D(S_z^A - S_z^B) & 0 & E_- + \frac{1}{2}M(S_z^A + S_z^B) \end{pmatrix}. \quad (D1)$$

The spectral problem is easily solved. Only the ground-state energy is presented here for both the $\uparrow\uparrow$ ($S_z^A + S_z^B = 1, S_z^A - S_z^B = 0$) and $\uparrow\downarrow$ ($S_z^A + S_z^B = 0, S_z^A - S_z^B = 1$) configurations,

$$E_{gs}(\uparrow\uparrow) = E_+(R) - \frac{1}{2}|P(R)|, \quad E_{gs}(\uparrow\downarrow) = \frac{E_+(R) + E_-(R)}{2} - \frac{1}{2}\sqrt{[E_+(R) - E_-(R)]^2 + D^2(R)}. \quad (D2)$$

In the case of intermediate and low interionic distances R , when the condition $|A| \ll |E_-(R) - E_+(R)|$ is fulfilled, the last formula is simplified,

$$E_{gs}(\uparrow\downarrow) = E_+(R) - \frac{D^2(R)}{4[E_-(R) - E_+(R)]},$$

that corresponds to the second-order perturbation theory.

The $\uparrow\uparrow$ configuration corresponds to lower energy regardless of the sign of the intracenter exchange parameter A , i.e., there is FM alignment.

2. Magnetic D_2^0 complex

For the magnetic D_2^0 complex, the 4×4 Hamiltonian is given by

$$H^{D_2^0}(S_z^A, S_z^B) = \begin{pmatrix} E_t - \xi(S_z^A + S_z^B) & 0 & 0 & 0 \\ 0 & E_t & 0 & -\zeta(S_z^A - S_z^B) \\ 0 & 0 & E_t + \xi(S_z^A + S_z^B) & 0 \\ 0 & -\zeta(S_z^A - S_z^B) & 0 & E_s \end{pmatrix}. \quad (D3)$$

This operator is written using the following order of basis vectors: $|1, +1\rangle, |1, 0\rangle, |1, -1\rangle$, and $|0, 0\rangle$. The ground-state energy for $\uparrow\uparrow$ and $\uparrow\downarrow$ d -shell configurations is given by

$$E_{gs}(\uparrow\uparrow) = E_s(R), \quad E_{gs}(\uparrow\downarrow) = E_s(R) - \frac{\zeta^2(R)}{E_t(R) - E_s(R)}, \quad (D4)$$

respectively. The second-order perturbation theory is also used here. The ground state corresponds to the AFM alignment (the $\uparrow\downarrow$ configuration has lower energy) regardless of the sign of the A parameter.

-
- [1] C. Zener, Interaction between the d shells in the transition metals, *Phys. Rev.* **81**, 440 (1951).
 [2] M. A. Ruderman and C. Kittel, Indirect exchange coupling of nuclear magnetic moments by conduction electrons, *Phys. Rev.* **96**, 99 (1954).
 [3] T. Kasuya, A theory of metallic ferro- and antiferromagnetism on Zener's model, *Prog. Theor. Phys.* **16**, 45 (1956).
 [4] K. Yosida, Magnetic properties of Cu-Mn alloys, *Phys. Rev.* **106**, 893 (1957).

- [5] T. Dietl, H. Ohno, F. Matsukura, J. Cibert, and D. Ferrand, Zener model description of ferromagnetism in Zinc-Blende magnetic semiconductors, *Science* **287**, 1019 (2000).
 [6] T. Dietl, H. Ohno, and F. Matsukura, Hole-mediated ferromagnetism in tetrahedrally coordinated semiconductors, *Phys. Rev. B* **63**, 195205 (2001).
 [7] F. Maca and J. Mařek, Electronic states in $\text{Ga}_{1-x}\text{Mn}_x\text{As}$: Substitutional versus interstitial position of Mn, *Phys. Rev. B* **65**, 235209 (2002).

- [8] K. M. Yu, W. Walukiewicz, T. Wojtowicz, I. Kuryliszyn, X. Liu, Y. Sasaki, and J. K. Furdyna, Effect of the location of Mn sites in ferromagnetic $\text{Ga}_{1-x}\text{Mn}_x\text{As}$ on its Curie temperature, *Phys. Rev. B* **65**, 201303(R) (2002).
- [9] H. Ohno, Properties of ferromagnetic III–V semiconductors, *J. Magn. Magn. Mater.* **200**, 110 (1999).
- [10] A. Oiwa, S. Katsumoto, A. Endo, M. Hirasawa, Y. Iye, H. Ohno, F. Matsukura, A. Shen, and Y. Sugawara, Nonmetal-metal-nonmetal transition and large negative magnetoresistance in $(\text{Ga}, \text{Mn})\text{As}/\text{GaAs}$, *Solid State Commun.* **103**, 209 (1997).
- [11] F. Matsukura, H. Ohno, A. Shen, and Y. Sugawara, Transport properties and origin of ferromagnetism in $(\text{Ga}, \text{Mn})\text{As}$, *Phys. Rev. B* **57**, R2037 (1998).
- [12] G. V. Astakhov, H. Hoffmann, V. L. Korenev, T. Kiessling, J. Schwitek, G. M. Schott, C. Gould, W. Ossau, K. Brunner, and L. W. Molenkamp, Nonthermal photoconcoercivity effect in a low-doped $(\text{Ga}, \text{Mn})\text{As}$ ferromagnetic semiconductor, *Phys. Rev. Lett.* **102**, 187401 (2009).
- [13] J. Linder and J. W. A. Robinson, Superconducting spintronics, *Nat. Phys.* **11**, 307 (2015).
- [14] A. S. Mel'nikov, S. V. Mironov, A. V. Samokhvalov, and A. I. Buzdin, Superconducting spintronics: state of the art and prospects, *Phys. Usp.* **65**, 1248 (2022).
- [15] F. S. Bergeret, A. F. Volkov, and K. B. Efetov, Odd triplet superconductivity and related phenomena in superconductor-ferromagnet structures, *Rev. Mod. Phys.* **77**, 1321 (2005).
- [16] P. G. De Gennes, Coupling between ferromagnets through a superconducting layer, *Phys. Lett.* **23**, 10 (1966).
- [17] N. S. Averkiev and A. A. Gutkin, Mn_{Ga} acceptor center in GaAs (Review), *Phys. Solid State* **60**, 2311 (2018).
- [18] I. A. Kokurin, P. V. Petrov, and N. S. Averkiev, Optical orientation of electrons in compensated semiconductors, *Semiconductors* **47**, 1232 (2013).
- [19] P. V. Petrov, I. A. Kokurin, Yu. L. Ivanov, N. S. Averkiev, R. P. Campion, B. L. Gallagher, P. M. Koenraad, and A. Yu. Silov, Optical orientation of spins in $\text{GaAs:Mn}/\text{AlGaAs}$ quantum wells via impurity-to-band excitation, *Phys. Rev. B* **94**, 085308 (2016).
- [20] I. A. Kokurin and N. S. Averkiev, Level structure of hole two-center complex and related luminescence in semiconductors, *Phys. Rev. B* **107**, 125208 (2023).
- [21] I. A. Kokurin and N. S. Averkiev, On a shape of band-to-acceptor luminescence line in semiconductors, *Bull. Russ. Acad. Sci.: Phys.* **87**, 744 (2023).
- [22] I. A. Kokurin, A. Yu. Silov, and N. S. Averkiev, Sign-reversal electron magnetization in Mn-doped semiconductor structures, *Phys. Rev. B* **102**, 041202(R) (2020).
- [23] T. Dietl and H. Ohno, Dilute ferromagnetic semiconductors: Physics and spintronic structures, *Rev. Mod. Phys.* **86**, 187 (2014).
- [24] T. O. Strandberg, C. M. Canali, and A. H. MacDonald, Magnetic interactions of substitutional Mn pairs in GaAs, *Phys. Rev. B* **81**, 054401 (2010).
- [25] M. Berciu and R. N. Bhatt, Effects of disorder on ferromagnetism in diluted magnetic semiconductors, *Phys. Rev. Lett.* **87**, 107203 (2001).
- [26] R. N. Bhatt, M. Berciu, M. P. Kennett, and X. Wan, Diluted magnetic semiconductors in the low carrier density regime, *J. Supercond. Nov. Magn.* **15**, 71 (2002).
- [27] M. Mayr, G. Alvarez, and E. Dagotto, Global versus local ferromagnetism in a model for diluted magnetic semiconductors studied with Monte Carlo techniques, *Phys. Rev. B* **65**, 241202(R) (2002).
- [28] M. P. Kennett, M. Berciu, and R. N. Bhatt, Monte Carlo simulations of an impurity-band model for III-V diluted magnetic semiconductors, *Phys. Rev. B* **66**, 045207 (2002).
- [29] N. O. Lipari and A. Baldereschi, Angular momentum theory and localized states in solids. Investigation of shallow acceptor states in semiconductors, *Phys. Rev. Lett.* **25**, 1660 (1970).
- [30] B. L. Gel'mont and M. I. D'yakov, Acceptor levels in diamond-type semiconductors, *Sov. Phys. Semicond.* **5**, 1905 (1972).
- [31] N. S. Averkiev and S. Yu. Il'inskii, Spin ordering of carriers localized on two deep centers in cubic semiconductors, *Phys. Solid State* **36**, 278 (1994).
- [32] J. C. Slater, *Quantum Theory of Molecules and Solids. Vol. 1: Electronic Structure of Molecules* (McGraw-Hill, New York, 1963).
- [33] I. N. Levine, *Quantum Chemistry*, 4th ed. (Prentice Hall, New Jersey, 1991).
- [34] P. W. Atkins and R. S. Friedman, *Molecular Quantum Mechanics* (Oxford University Press, New York, 2011).
- [35] The problem can also be solved using the well-known Heitler-London scheme. However, the ground state of H_2 molecule, calculated in MO-LCAO approximation, has a value closer to experimental one. This is due to taking into account the mixing of the Ψ_1 and Ψ_4 states that in quantum chemistry is usually called configuration interaction. It should be noted that the Heitler-London approach does not take into account the so-called ionic contributions to the wave functions, i.e., the possibility of localization of both electrons at the same nucleus is neglected.
- [36] The internal structure of the d shell is not considered here. Those interested can refer to the recent paper [59], where this topic is covered as well as the change of the exchange strength due to thermal expansion or external strain of the crystal.
- [37] This representation of the exchange operator corresponds to first-order perturbation theory with respect to the small parameter $|A|/E_0 \ll 1$. The next-order correction to the exchange parameter due to the coupling with the ns hydrogen-like states ($n = 2, 3, \dots$) is easy to estimate, $-\frac{A^2}{E_0} \sum_{n=2}^{\infty} \frac{1}{n(n^2-1)} = -\frac{1}{4} \frac{A^2}{E_0}$. The known sum of the series is used here [60], $\sum_{k=1}^{\infty} \frac{1}{k(k+1)(k+2)} = \frac{1}{4}$.
- [38] W. Nolting and A. Ramakanth, *Quantum Theory of Magnetism* (Springer-Verlag, Berlin, 2009).
- [39] H. A. Bethe and E. E. Salpeter, *Quantum Mechanics of One- and Two-Electron Atoms* (Plenum Publishing, New York, 1977).
- [40] N. A. Bogoslovskiy, P. V. Petrov, and N. S. Averkiev, The impurity magnetic susceptibility of semiconductors in the case of direct exchange interaction in the Ising model, *Phys. Solid State* **61**, 2005 (2019).
- [41] N. A. Bogoslovskiy, P. V. Petrov, and N. S. Averkiev, Spin-fluctuation transition in the disordered Ising model, *JETP Lett.* **114**, 347 (2021).
- [42] N. A. Bogoslovskiy, P. V. Petrov, and N. S. Averkiev, Phase diagram of a ferromagnetic semiconductor: Origin of superparamagnetism, *Phys. Rev. B* **109**, 024436 (2024).
- [43] The interstitial Mn_I is a double donor. When there is one interstitial Mn_I atom per three substitutional Mn_{Ga} acceptors

- (Mn interstitials amount is 25% of the total manganese content), the electrons supplied by Mn_I transfer two acceptors to the ionized Mn_{Ga}^- state. The high mobility of the interstitial Mn_I^{2+} ion and Coulomb attraction allow it to occupy the position close to the ionized Mn_{Ga}^- center. The so-called magnetic compensation occurs [44]: the d shells in $\text{Mn}_{\text{Ga}} - \text{Mn}_I$ pairs are aligned antiferromagnetically, as a result, the number of magnetic moments participating in ferromagnetism decreases. Finally, ionized Mn_{Ga}^- and neutral Mn_{Ga}^0 acceptors are in equal numbers, that is necessary for FM ordering.
- [44] J. K. Furdyna, X. Liu, M. Dobrowolska, and S. Lee, Mn impurity band and the effects of Mn position in III–V lattice: Pivotal contributions of Władek Walukiewicz to the understanding of ferromagnetism in semiconductors, *J. Appl. Phys.* **134**, 200901 (2023).
- [45] Y. J. Cho, X. Liu, and J. K. Furdyna, Collapse of ferromagnetism in (Ga, Mn)As at high hole concentrations, *Semicond. Sci. Technol.* **23**, 125010 (2008).
- [46] M. Dobrowolska, K. Tivakornsasithorn, X. Liu, J. K. Furdyna, M. Berciu, K. M. Yu, and W. Walukiewicz, Controlling the Curie temperature in (Ga,Mn)As through location of the Fermi level within the impurity band, *Nat. Mater.* **11**, 444 (2012).
- [47] S. C. Erwin and A. G. Petukhov, Self-compensation in manganese-doped ferromagnetic semiconductors, *Phys. Rev. Lett.* **89**, 227201 (2002).
- [48] S. Blundell, *Magnetism in Condensed Matter* (Oxford University Press, Oxford, 2001).
- [49] I. Vurgaftman, J. R. Meyer, and L. R. Ram-Mohan, Band parameters for III–V compound semiconductors and their alloys, *J. Appl. Phys.* **89**, 5815 (2001).
- [50] N. S. Averkiev, A. A. Gutkin, E. B. Osipov, and M. A. Reshchikov, Effect of the exchange interaction of a hole with $3d$ electrons on the properties of a deep Mn acceptor in gallium arsenide, *Sov. Phys. Solid State* **30**, 438 (1988).
- [51] Th. Frey, M. Maier, J. Schneider, and M. Gehrke, Paramagnetism of the manganese acceptor in gallium arsenide, *J. Phys. C: Solid State Phys.* **21**, 5539 (1988).
- [52] M. Linnarsson, E. Janzén, B. Monemar, M. Kleverman, and A. Thilderkvist, Electronic structure of the GaAs:Mn_{Ga} center, *Phys. Rev. B* **55**, 6938 (1997).
- [53] V. F. Sapega, T. Ruf, and M. Cardona, Spin-Flip Raman study of exchange interactions in bulk GaAs:Mn, *Phys. Status Solidi B* **226**, 339 (2001).
- [54] A. K. Bhattacharjee and C. Benoit à la Guillaume, Model for the Mn acceptor in GaAs, *Solid State Commun.* **113**, 17 (1999).
- [55] If the compensation is provided by Mn_I donors then concentration x_{eff} of magnetic moments contributing to the FM order is equal to the difference between the concentration of the substitutional Mn (x_s) and interstitials (x_i) [46], $x_{\text{eff}} = x_s - x_i$. The total Mn concentration is equal to $x = x_s + x_i$. Thus, $x_{\text{eff}} = x - 2x_i$, and the ionized and neutral substitutional Mn acceptors, contributing to FM ordering, have equal concentrations $x/4$ (their total concentration $x_{\text{eff}} = x/2$) if $x_i = x/4$.
- [56] The Bohr radius of 1 nm corresponds to the binding energy of the Coulomb center $\frac{e^2}{2\epsilon a_B} = 55.8$ meV (a value of 12.9 is used for the static dielectric constant ϵ of GaAs), i.e., the contribution of the central cell correction to the binding energy is approximately half, $96.9 - 55.8 = 41.1$ meV.
- [57] A. C. Durst, K. E. Castoria, and R. N. Bhatt, Heitler-London model for acceptor-acceptor interactions in doped semiconductors, *Phys. Rev. B* **96**, 155208 (2017).
- [58] M. Abramowitz and I. A. Stegun, *Handbook of Mathematical Functions* (Dover, New York, 1964).
- [59] I. V. Krainov, K. A. Baryshnikov, A. A. Karpova, and N. S. Averkiev, Exchange interaction for Mn acceptors in GaAs: Revealing its strong deformation dependence, *Phys. Rev. B* **107**, 174401 (2023).
- [60] A. P. Prudnikov, Yu. A. Brychkov, and O. I. Marichev, *Integrals and Series, Vol. 1: Elementary Functions* (Gordon and Breach, New York, 1986).